



Cranial morphology and phylogenetic relationships of Amynodontidae Scott and Osborn, 1883 (Perissodactyla, Rhinocerotoidea)

Lea Veine-Tonizzo, Jérémie Tissier, Maia Bukhsianidze, Davit Vasilyan,
Damien Becker

► To cite this version:

Lea Veine-Tonizzo, Jérémie Tissier, Maia Bukhsianidze, Davit Vasilyan, Damien Becker. Cranial morphology and phylogenetic relationships of Amynodontidae Scott and Osborn, 1883 (Perissodactyla, Rhinocerotoidea). Comptes Rendus. Palevol, 2023, 22 (8), pp.109-142. 10.5852/cr-palevol2023v22a8 . hal-04090054

HAL Id: hal-04090054

<https://hal.science/hal-04090054>

Submitted on 5 May 2023

HAL is a multi-disciplinary open access archive for the deposit and dissemination of scientific research documents, whether they are published or not. The documents may come from teaching and research institutions in France or abroad, or from public or private research centers.

L'archive ouverte pluridisciplinaire **HAL**, est destinée au dépôt et à la diffusion de documents scientifiques de niveau recherche, publiés ou non, émanant des établissements d'enseignement et de recherche français ou étrangers, des laboratoires publics ou privés.



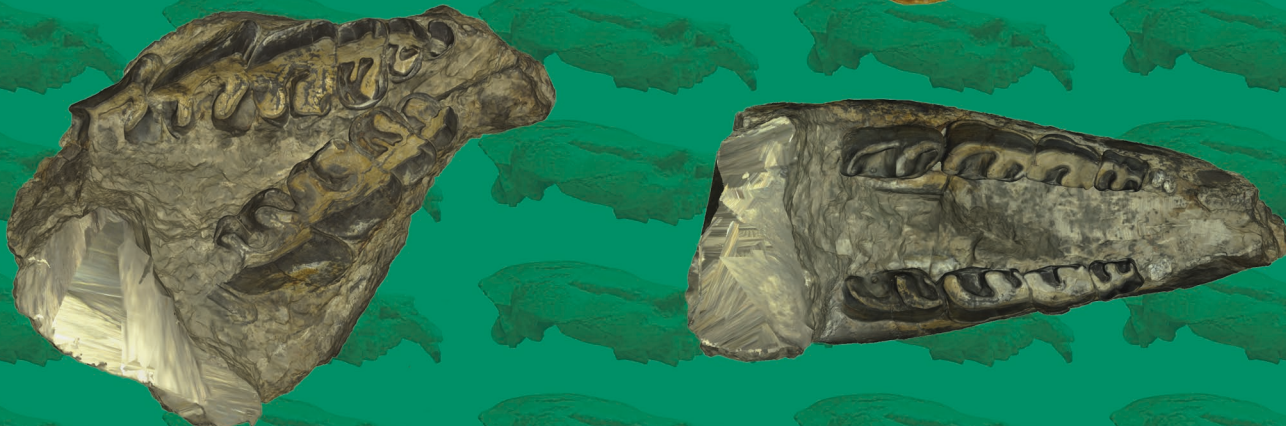
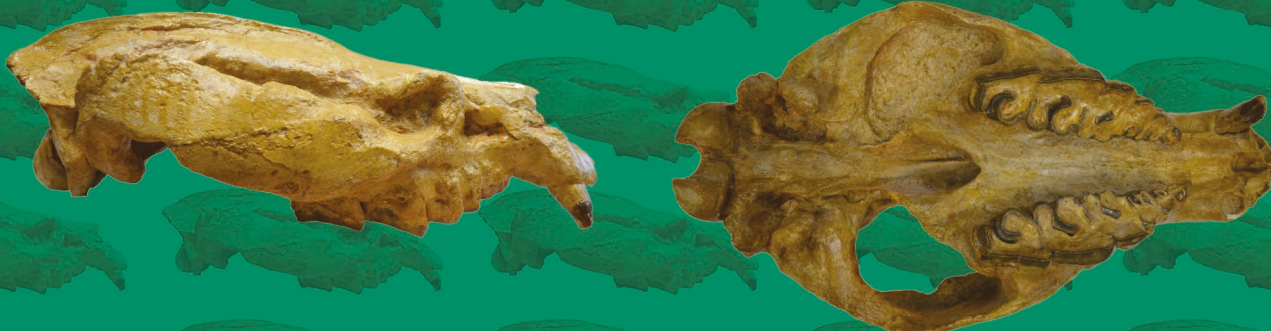
Distributed under a Creative Commons Attribution 4.0 International License

comptes rendus palevol

2023 • 22 • 8

Cranial morphology and phylogenetic relationships of Amynodontidae Scott & Osborn, 1883 (Perissodactyla, Rhinocerotoidea)

Léa VEINE-TONIZZO, Jérémie TISSIER, Maia BUKHSIANIDZE,
Davit VASILYAN & Damien BECKER



art. 22 (8) — Published on 20 March 2023
www.cr-palevol.fr



PUBLICATIONS
SCIENTIFIQUES



DIRECTEURS DE LA PUBLICATION / *PUBLICATION DIRECTORS*:

Bruno David, Président du Muséum national d'Histoire naturelle
Étienne Ghys, Secrétaire perpétuel de l'Académie des sciences

RÉDACTEURS EN CHEF / *EDITORS-IN-CHIEF*: Michel Laurin (CNRS), Philippe Taquet (Académie des sciences)

ASSISTANTE DE RÉDACTION / *ASSISTANT EDITOR*: Adenise Lopes (Académie des sciences; cr-palevol@academie-sciences.fr)

MISE EN PAGE / *PAGE LAYOUT*: Audrina Neveu (Muséum national d'Histoire naturelle; audrina.neveu@mnhn.fr)

RÉVISIONS LINGUISTIQUES DES TEXTES ANGLAIS / *ENGLISH LANGUAGE REVISIONS*: Kevin Padian (University of California at Berkeley)

RÉDACTEURS ASSOCIÉS / *ASSOCIATE EDITORS* (*, took charge of the editorial process of the article/a pris en charge le suivi éditorial de l'article):

Micropaléontologie/*Micropalaeontology*

Maria Rose Petrizzo (Università di Milano, Milano)

Paléobotanique/*Palaeobotany*

Cyrille Prestianni (Royal Belgian Institute of Natural Sciences, Brussels)

Métazoaires/*Metazoa*

Annalisa Ferretti (Università di Modena e Reggio Emilia, Modena)

Paléoichthyologie/*Palaeoichthyology*

Philippe Janvier (Muséum national d'Histoire naturelle, Académie des sciences, Paris)

Amniotes du Mésozoïque/*Mesozoic amniotes*

Hans-Dieter Sues (Smithsonian National Museum of Natural History, Washington)

Tortues/*Turtles*

Walter Joyce (Universität Freiburg, Switzerland)

Lépidosauromorphes/*Lepidosauromorphs*

Hussam Zaher (Universidade de São Paulo)

Oiseaux/*Birds*

Eric Buffetaut (CNRS, École Normale Supérieure, Paris)

Paléomammalogie (mammifères de moyenne et grande taille)/*Palaeomammalogy (large and mid-sized mammals)*

Lorenzo Rook* (Università degli Studi di Firenze, Firenze)

Paléomammalogie (petits mammifères sauf Euarchontoglires)/*Palaeomammalogy (small mammals except for Euarchontoglires)*

Robert Asher (Cambridge University, Cambridge)

Paléomammalogie (Euarchontoglires)/*Palaeomammalogy (Euarchontoglires)*

K. Christopher Beard (University of Kansas, Lawrence)

Paléoanthropologie/*Palaeoanthropology*

Aurélien Mounier (CNRS/Muséum national d'Histoire naturelle, Paris)

Archéologie préhistorique (Paléolithique et Mésolithique)/*Prehistoric archaeology (Palaeolithic and Mesolithic)*

Nicolas Teyssandier (CNRS/Université de Toulouse, Toulouse)

Archéologie préhistorique (Néolithique et âge du bronze)/*Prehistoric archaeology (Neolithic and Bronze Age)*

Marc Vander Linden (Bournemouth University, Bournemouth)

RÉFÉRÉS / *REVIEWERS*: <https://sciencepress.mnhn.fr/fr/periodiques/comptes-rendus-palevol/referes-du-journal>

COUVERTURE / *COVER*:

Made from the Figures of the article.

Comptes Rendus Palevol est indexé dans / *Comptes Rendus Palevol* is indexed by:

- Cambridge Scientific Abstracts
- Current Contents® Physical
- Chemical, and Earth Sciences®
- ISI Alerting Services®
- Geoabstracts, Geobase, Georef, Inspec, Pascal
- Science Citation Index®, Science Citation Index Expanded®
- Scopus®.

Les articles ainsi que les nouveautés nomenclaturales publiés dans *Comptes Rendus Palevol* sont référencés par /
Articles and nomenclatural novelties published in Comptes Rendus Palevol are registered on:

- ZooBank® (<http://zoobank.org>)

Comptes Rendus Palevol est une revue en flux continu publiée par les Publications scientifiques du Muséum, Paris et l'Académie des sciences, Paris
Comptes Rendus Palevol is a fast track journal published by the Museum Science Press, Paris and the Académie des sciences, Paris

Les Publications scientifiques du Muséum publient aussi / The Museum Science Press also publish:

Adansonia, *Geodiversitas*, *Zoosystema*, *Anthropozoologica*, *European Journal of Taxonomy*, *Naturae*, *Cryptogamie* sous-sections *Algologie*, *Bryologie*, *Mycologie*.

L'Académie des sciences publie aussi / The Académie des sciences also publishes:

Comptes Rendus Mathématique, *Comptes Rendus Physique*, *Comptes Rendus Mécanique*, *Comptes Rendus Chimie*, *Comptes Rendus Géoscience*, *Comptes Rendus Biologies*.

Diffusion – Publications scientifiques Muséum national d'Histoire naturelle

CP 41 – 57 rue Cuvier F-75231 Paris cedex 05 (France)

Tél.: 33 (0)1 40 79 48 05 / Fax: 33 (0)1 40 79 38 40

diff.pub@mnhn.fr / <https://sciencepress.mnhn.fr>

Académie des sciences, Institut de France, 23 quai de Conti, 75006 Paris.

© This article is licensed under the Creative Commons Attribution 4.0 International License (<https://creativecommons.org/licenses/by/4.0/>)

ISSN (imprimé / print): 1631-0683/ ISSN (électronique / electronic): 1777-571X

Cranial morphology and phylogenetic relationships of Amynodontidae Scott & Osborn, 1883 (Perissodactyla, Rhinocerotoidea)

Léa VEINE-TONIZZO

Géosciences Rennes, UMR 6118, Université de Rennes 1, CNRS, 35000 Rennes (France)
and JURASSICA Museum, Route de Fontenais 21, CH-2900 Porrentruy (Switzerland)
and Department of Earth Sciences, Carleton University, 1125 Colonel By Drive,
Ottawa, ON, K1S 5B6 (Canada)
and Beaty Centre for Species Discovery, Canadian Museum of Nature,
PO Box 3443, Station D., Ottawa, ON, K1P 6P4 (Canada)
leaveinetonizzo@cmail.carleton.ca (corresponding author)

Jérémy TISSIER

JURASSICA Museum, Route de Fontenais 21, CH-2900 Porrentruy (Switzerland)
and American Museum of Natural History, Central Park West at 79th Street,
US-10024 New York (United States)
jeremy.tissier123@gmail.com

Maia BUKHSIANIDZE

Georgian National Museum, 3, Purtseladze street, Tbilisi 0105 (Georgia)
maiabukh@gmail.com

Davit VASILYAN
Damien BECKER

JURASSICA Museum, Route de Fontenais 21, CH-2900 Porrentruy (Switzerland)
and Department of Geosciences, University of Fribourg, CH-1700 Fribourg (Switzerland)
davit.vasilyan@jurassica.ch
damien.becker@jurassica.ch

Submitted on 2 February 2021 | Accepted on 27 January 2022 | Published on 20 March 2023

[urn:lsid:zoobank.org:pub:3201699E-0180-4DB2-9C25-60EE6A783D85](https://doi.org/10.5852/cr-palevol2023v22a8)

Veine-Tonizzo L., Tissier J., Bukhsianidze M., Vasilyan D. & Becker D. 2023. — Cranial morphology and phylogenetic relationships of Amynodontidae Scott & Osborn, 1883 (Perissodactyla, Rhinocerotoidea). *Comptes Rendus Palevol* 22 (8): 109-142. <https://doi.org/10.5852/cr-palevol2023v22a8>

ABSTRACT

Amynodontidae Scott & Osborn, 1883 are an extinct family of Rhinocerotoidea Owen, 1845 known from the middle Eocene to the latest Oligocene of Asia, North America, and Europe. We report here two unpublished specimens of Amynodontidae, a skull and a mandible of *Zaisanamynodon borisovi* Belyaeva, 1971 from the late Eocene of the Zaysan Basin (Kazakhstan) and a skull of *Metamynodon planifrons* Scott & Osborn, 1887, from the early Oligocene of the Big Badlands (United States). This new material has been incorporated into a morpho-anatomical character matrix. It was completed with the coding of the recently described species of *Amynodontopsis jiyuanensis* Wang X.-Y., Wang Y.-Q., Zhang R., Zhang Z.-H., Liu & Ren, 2020 and the revised coding of *Cadurcotherium*

KEY WORDS
 Amynodontidae,
Zaisanamynodon,
Metamynodon,
 phylogeny,
 skull,
 Zaysan Basin,
 Big Badlands,
 Eocene,
 Oligocene,
 Rhinocerotoidea.

MOTS CLÉS
 Amynodontidae,
Zaisanamynodon,
Metamynodon,
 phylogénie,
 crâne,
 Bassin Zaïssan,
 Big Badlands,
 Éocène,
 Oligocène,
 Rhinocerotoidea.

caylusi Gervais, 1873 and *Cadurcotherium minum* Filhol, 1880. We computed a cladistic analysis based on this matrix, including 31 Rhinocerotoidea terminal taxa. The new phylogenetic hypothesis proposed allows to discuss the relationships of the referred specimens within Amynodontidae and those of Amynodontidae within Rhinocerotoidea. Our cladistic analysis clarifies the generic and specific composition of the tribes Metamynodontini Kretzoi, 1942 and Cadurcodontini Wall, 1982 and supports the monophyly of the genus *Zaisanamynodon* Belyaeva, 1971. The dichotomy between the two tribes is notably expressed by the presence of several cranial features such as “the deep nasal notch” or “the well-developed preorbital fossa” in Cadurcodontini. These cranial specializations attest to an adaptation of the peri-nasal region to the presence of a proboscis with a feeding function. Our study also opens a discussion on the biogeography of Amynodontidae, their emergence and dispersal in Asia and their subsequent migration to North America, and Eastern Europe. Their presence in Western Europe remains restricted to the Oligocene, after a dispersal related to the “Grande Coupure” event.

RÉSUMÉ

Morphologie crânienne et relations phylogénétiques des Amynodontidae Scott & Osborn, 1883 (Perissodactyla, Rhinocerotoidea).

Les Amynodontidae Scott & Osborn, 1883 sont une famille éteinte de Rhinocerotoidea Owen, 1845 connue depuis l’Éocène moyen jusqu’à la fin de l’Oligocène en Asie, en Amérique du Nord et en Europe. Nous présentons ici deux spécimens inédits d’Amynodontidae, un crâne et une mandibule, de *Zaisanamynodon borisovi* Belyaeva, 1971, datés de la fin de l’Éocène du bassin de Zaïssan (Kazakhstan) et un crâne de *Metamynodon planifrons* Scott & Osborn, 1887, daté du début de l’Oligocène des Big Badlands (États-Unis). Ce nouveau matériel a été inclus dans une matrice de caractères morpho-anatomiques. Elle a été complétée par le codage de l’espèce récemment décrite *Amynodontopsis jiyuanensis* Wang X.-Y., Wang Y.-Q., Zhang R., Zhang Z.-H., Liu & Ren, 2020 et les codages révisés de *Cadurcotherium caylusi* Gervais, 1873 et *Cadurcotherium minum* Filhol, 1880. Nous avons réalisé une analyse cladistique basée sur cette matrice, incluant 31 taxons terminaux de Rhinocerotoidea. La nouvelle hypothèse phylogénétique proposée permet de discuter des positions phylogénétiques des spécimens étudiés au sein des Amynodontidae et de la position des Amynodontidae au sein des Rhinocerotoidea. Notre analyse cladistique clarifie la composition générique et spécifique des tribus Metamynodontini Kretzoi, 1942 et Cadurcodontini Wall, 1982 et soutient la monophylie de *Zaisanamynodon* Belyaeva, 1971. La dichotomie des deux tribus s’exprime notamment par la présence de plusieurs caractéristiques crâniennes telles que “l’allongement de l’incisure nasale” ou “la fosse préorbitaire bien développée” chez les Cadurcodontini. Ces spécialisations témoignent d’une adaptation de la région péri-nasale à la présence d’un proboscis. Notre étude ouvre également une discussion sur la biogéographie des Amynodontidae, leur émergence et dispersion en Asie à l’Éocène moyen puis leur colonisation de l’Amérique du Nord et de l’Europe de l’Est. Leur présence en Europe occidentale est, quant à elle, restreinte à l’Oligocène et liée à l’événement de la Grande Coupure.

INTRODUCTION

Amynodontidae Scott & Osborn, 1883 are an extinct family of hornless perissodactyls, which are included within Rhinocerotoidea Owen, 1845. They are assumed to be terrestrial herbivores but some of them were probably semi-aquatic (e.g. Wall 1982b, 1989, 1998; Wall & Heinbaugh 1999). They had a noticeable diversification during the middle and late Eocene in Asia and North America (e.g. Wall 1998; Averianov *et al.* 2016; Tissier *et al.* 2018). Amynodontidae were also present in Eastern Europe since the middle Eocene, and later during the Oligocene they are documented in Western Europe (e.g. Averianov *et al.* 2016; Tissier *et al.* 2018). This late dispersal would have been the consequence of establishment of land connections between Asia and Europe at the beginning of the Oligocene (i.e., the “Grande Coupure” event; Stehlin 1909; Legendre 1989; Hooker *et al.* 2004).

The monophyly of Amynodontidae is defined by well-supported synapomorphies such as the presence of a preorbital fossa, the loss of upper and lower P1, enlarged canines and the quadratic shape of the M3 (Wall 1980; Tissier *et al.* 2018). Relationships within Amynodontidae have been well studied since the 1940s (e.g. Wood 1941; Kretzoi 1942; Gromova 1954; Wall 1980). The first handmade phylogenetic analyses were performed by Wall (1982a, 1989, 1998) and, more recently, Averianov *et al.* (2016) and Tissier *et al.* (2018) published comprehensive phylogenies of the family based on computed cladistic analyses. Their new phylogenetic results led to a better understanding of the evolutionary history and the generic composition of the two major clades of the family: the Cadurcodontini Wall, 1982 and the Metamynodontini Scott & Osborn, 1887. Tissier *et al.* (2018) also underlined that suprageneric relationships within Rhinocerotoidea appear to be unclear, especially concerning

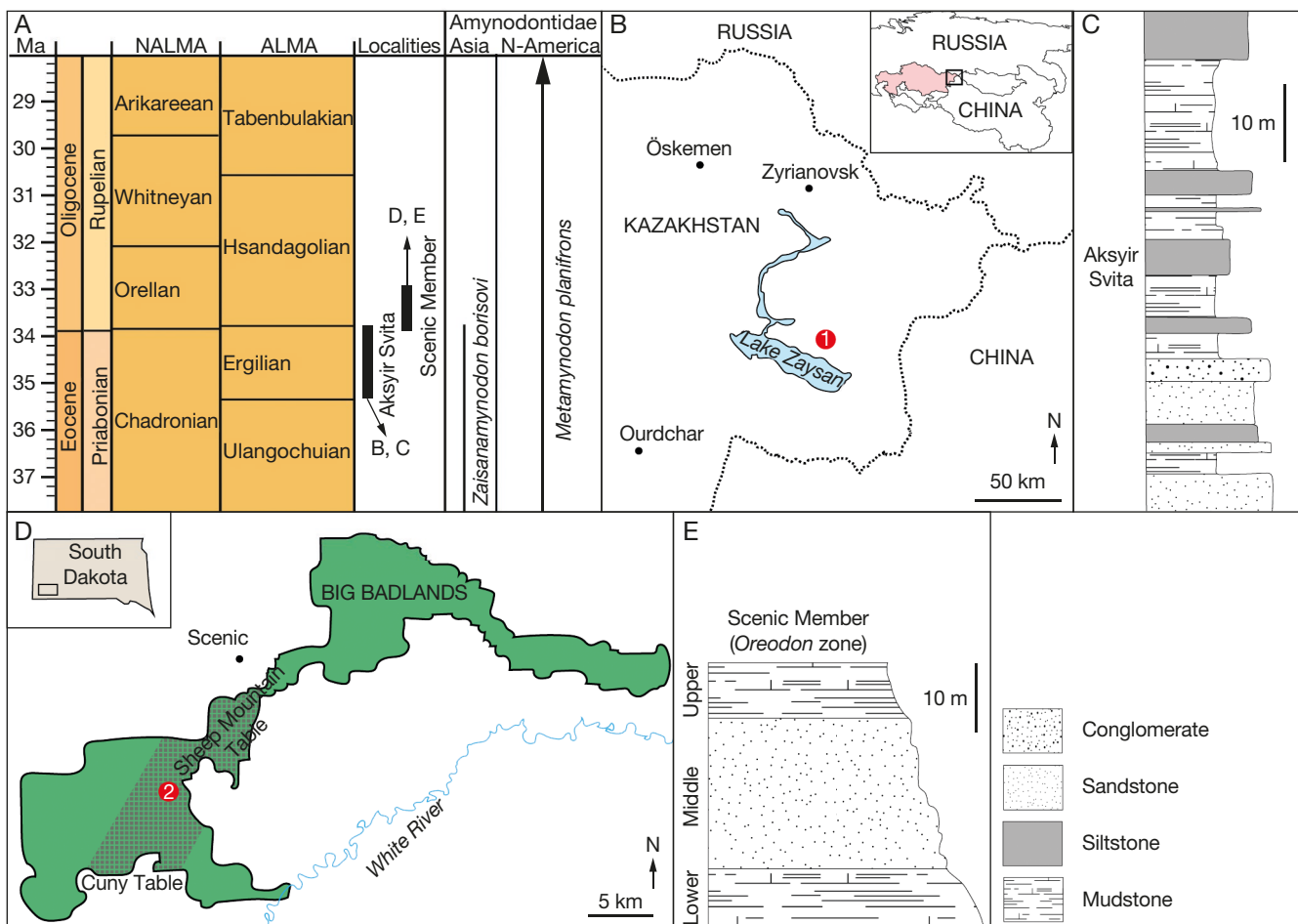


FIG. 1. — Biochronology, geography and stratigraphy information on cited localities: **A**, correlations between considered localities and temporal distributions of species described in the present paper; **B**, map of the area of the Lake Zaysan, Kazakhstan with locality of collect of ZSN-KKS-28-IPB; **C**, outcrop of the Aksyir Svita at Kiin Kerish (adapted from Lucas *et al.* 2012); **D**, map of Big Badlands, South Dakota, United States with supposed area of collect of UNISTRA.2015.0.1106; **E**, outcrop of the Scenic Member (Oreodon zone) of the Brule Formation of the White River Group (adapted from Benton *et al.* 2015). Numbers: 1, Kiin Kerish, locality of collect of ZSN-KKS-28-IPB ($48^{\circ}07'52.2''N$, $84^{\circ}28'52.3''E$); 2, supposed area of collect of UNISTRA.2015.0.11.06 (see Gillet 1960).

the “Hyracodontidae” Cope, 1879 and basal taxa of Amynodontidae. Indeed, the position of Amynodontidae within the Rhinocerotoidea is conflictual according to the most recent phylogenies. According to Wang *et al.* (2016, 2018) and Tissier *et al.* (2018), Amynodontidae would be the sister-group of the Paraceratheriidae Osborn, 1923, whereas according to Bai *et al.* (2020), they would be either sister-group of the clade formed by *Eggyodon* Roman, 1910, Paraceratheriidae and Rhinocerotidae Gray, 1821 based on a parsimony analysis, or sister-group of the Hyracodontidae, Eggyodontidae Breuning, 1923, Paraceratheriidae and Rhinocerotidae based on a Bayesian tip-dating analysis. Therefore, more data is necessary to better understand the early diversification of the main families of Rhinocerotoidea, which can be done by documenting their taxonomical and morphological diversity.

Here, we describe an unpublished skull and mandible (ZSN-KKS-28-IPB) of Amynodontidae from the late Eocene of the Zaysan Basin (Kazakhstan) and another amynodontid skull (UNISTRA.2015.0.1106) from the early Oligocene of the Big Badlands (United States). These specimens have been included in a parsimony analysis of a morphological characters matrix.

It includes a large sample of Rhinocerotoidea and a comprehensive amynodontid sampling. Our sampling aims to infer the phylogenetic positions of the referred specimens within Amynodontidae and the position of Amynodontidae within Rhinocerotoidea. The results are also discussed within the scope of the peculiar cranio-dental anatomy of the Amynodontidae and their biogeographical distribution.

MATERIAL AND METHODS

MATERIAL

The specimen ZSN-KKS-28-IPB, is a fragmented skull with P2-M3 in connection with a fragmented mandible with p4-m3. It was collected by Prof. Vyacheslav Chkhikvadze† in the 1980s and it is housed in the Georgian National Museum in Tbilisi, Georgia. The skull was found in the Kiin Kerish locality ($48^{\circ}07'52.2''N$, $84^{\circ}28'52.3''E$) from the north of the Lake Zaysan, Kazakhstan. The fossiliferous layer is related to the Aksyir Svita. This stratigraphical unit is correlated to the Ergilian Asian Land Mammal Age (ALMA) which corresponds

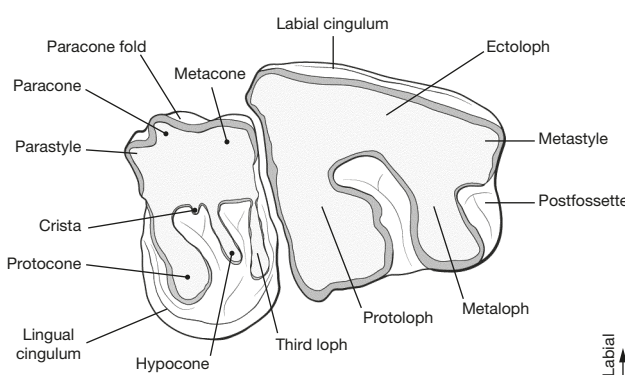
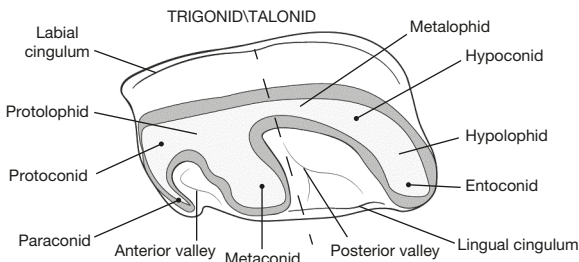
A**B**

FIG. 2. — Dental terminology used for Amynodontidae Scott & Osborn, 1883: **A**, left P4-M1, hypothetical; **B**, right m2, hypothetical. Scale bar: 1 cm.

to a late Eocene age (e.g. Russell & Zhai 1987; Lucas & Emry 1996; Emry *et al.* 1998; Lucas *et al.* 2012; Vandenberghe *et al.* 2012). The section of the Aksyir Sita at the Kiin Kerish locality is characterized by alternation of claystones, siltstones, sandstones (Borisov 1963; Lucas *et al.* 2012), which most probably represent fluvio-lacustrine deposits (Fig. 1A-C).

The specimen UNISTRA.2015.0.1106, is a well-preserved skull with right C1 and both P2-M3 series. It is housed in the collections of the “École et observatoire des sciences de la terre de Strasbourg”, Université de Strasbourg, France, and it was briefly described for the first time in Gillet *et al.* (1957) and then in Gillet (1960). UNISTRA.2015.0.1106 was found in southwestern South Dakota at the Big Badlands National Park, United States. It was collected in the mudstone beds of the lower part of the Scenic Member (*Oreodon* zone) of the Brule Formation of the White River Group somewhere between the Sheep Mountain Table and the Cuny Table (Gillet 1960; for further information about the White River Group see Benton *et al.* 2015). The mudstone beds of the lower part of the Scenic Member (*Oreodon* zone) are dated from the early Orellan North America Land Mammal Age (NALMA) and correspond to an early Oligocene age (Gillet 1960; Prothero & Emry 2004, Benton *et al.* 2015) (Fig. 1A, D, E).

SURFACE SCANNING

Specimens were scanned with a structured-light surface scanner (Artec Space Spider) and the three-dimensional models were reconstructed using the Artec Studio 13 Professional software. The three-dimensional model of the specimen UNISTRA.2015.0.1106 is available in Veine-Tonizzo *et al.* (2023).

MEASUREMENTS AND ANATOMICAL TERMINOLOGY

Dental terminology used is illustrated in Figure 2. Cranial terminology is from Antoine (2002). Dental measurements are taken according to Uhlig (1999). Measurements are given in millimeters, and they are in parentheses when estimated.

PHYLOGENETIC ANALYSIS

The matrix consisted of 32 terminals scored across 298 anatomical characters (Appendix 1). It is mainly based on the variation by Tissier *et al.* (2018) of the character matrix by Antoine (2002). The sample of terminals consists of twenty-seven taxa previously coded (Antoine *et al.* 2010; Tissier *et al.* 2018), including *Tapirus terrestris* (Von Linnaeus, 1758) and *Hyrachys eximus* Leidy, 1871 considered as outgroups for this analysis, eleven terminals forming the branching-group (*sensu* Antoine, 2002) composed of major groups of Rhinocerotoidea (i.e., early Rhinocerotoidea; Rhinocerotidae; “Hyracodontidae”: Eggysodontidae, Paraceratheriidae), and fourteen terminals of Amynodontidae Scott & Osborn, 1883. The sample also includes three new terminals of Amynodontidae: *Amynodontopsis jiyuanensis* Wang X.-Y., Wang Y.-Q., Zhang R., Zhang Z.-H., Liu & Ren, 2020, ZSN-KKS-28-IPB and UNISTRA.2015.0.1106. Additionally, the coding of *Cadurcotherium cayluxi* Gervais, 1873 and *Cadurcotherium minum* Filhol, 1880 were revised based on the recent publication of Ménouret (2018). The phylogeny of the Amynodontidae was recently revised by Averianov *et al.* (2016) and Tissier *et al.* (2018). The sample of terminals of this study was chosen to test the latter results by including the new referred specimens and the revised coding of *Cadurcotherium* Gervais, 1873 within Amynodontidae (Table 1). Hence, the cladistic analysis does not intend to resolve the full phylogeny of Rhinocerotoidea.

The complete list of characters used is available in Appendix 2. Character's coding is based on direct observations of specimens and/or on publications (photographs, descriptions, and illustrations). Italicized numbers refer to character numbers, their associate state is in parentheses.

The matrix is composed of the characters 1-282 from the sequence of Antoine (2002), including the characters 36, 60, 103 and 140 modified from the original sequence to form morphoclines by Tissier *et al.* (2018). The characters 283-289 are from the matrix of Tissier *et al.* (2018). The characters 290-297 are based on the characters 8, 9, 16, 23, 25, 39, 41 and 45 of Averianov *et al.* (2016). The character 298 is newly included here: P4 third posterior loph = 0, absent; 1, present.

The cladistic analysis was computed with the traditional search in TNT version 1.5 (Goloboff *et al.* 2008) and the heuristic search in PAUP* version 4.0a167 (Swofford 2002). In TNT, starting trees were obtained from Wagner trees. Thousand replications of addition-sequence were performed using the tree bisection reconnection (TBR) algorithm and saving ten trees per replicate. In PAUP*, starting trees for branch-swapping were obtained by stepwise addition sequence of 1000 random replicates, holding ten trees at each step.

Branch-swapping was run with the TBR algorithm and the MulTrees option. Decay Index (Bremer support) was calculated with the use of TreeRot.v3 (Sorenson & Franzosa 2007) and PAUP*. Bootstrap, consistency index (CI) and retention index (RI) were calculated with PAUP*.

ABBREVIATIONS

Institutions

AMNH	American Museum of Natural History, New York;
ANPIN	Palaeontological Institute of the Russian Academy of Sciences, Moscow;
IPB	former L. Davitashvili Institute of Palaeobiology, Tbilisi now part of the Georgian National Museum, Tbilisi;
MJSN	Jurassica Museum (formerly “Musée jurassien des sciences naturelles”), Porrentruy;
UNISTRA	Collections of the “École et observatoire des sciences de la terre de Strasbourg”, Université de Strasbourg;
VPM	Vertebrate Paleontology Mammal collection of the Museum of Comparative Zoology of Harvard University, Cambridge.

Measurements

H	height;
L	length;
W	width.

Dental

c/C	lower/upper canine;
i/I	lower/upper incisor;
m/M	lower/upper molar;
p/P	lower/upper premolar.

Other

ALMA	Asian Land Mammal Age;
CI	consistency index;
NALMA	North America Land Mammal Age;
RI	retention index;
TBR	Tree bisection reconnection.

SYSTEMATIC PALAEONTOLOGY

Class MAMMALIA Linnaeus, 1758
 Order PERISSODACTYLA Owen, 1848
 Superfamily RHINOCEROTOIDEA Gray, 1821
 Family AMYNODONTIDAE Scott & Osborn, 1883
 Tribe CADURCODONTINI Wall, 1982

Genus *Zaisanamynodon* Belyaeva, 1971

Procadurcodon Gromova (*Nomen nudum*) 1960: 129.

Zaisanamynodon Belyaeva, 1971: 43.

TYPE SPECIES. — *Zaisanamynodon borisovi* Belyaeva, 1971.

INCLUDED SPECIES. — *Zaisanamynodon protheroi* Lucas, 2006.

EMENDED DIAGNOSIS. — Within Cadurcodontini, *Zaisanamynodon* differs from other genera (*Cadurcotherium*, *Amynodontopsis* Stock, 1933, and *Cadurcodon* Kretzoi, 1942) by the presence of a third

posterior loph on P4. *Zaisanamynodon* differs from *Cadurcotherium* by the absence of cement on cheek teeth, an oblique hypolophid on lower molars and a long metastyle on M1-2. *Zaisanamynodon* differs from *Amynodontopsis* in having a postfossette on M1 and the absence of a sagittal crest on the basilar process. *Zaisanamynodon* differs from *Cadurcodon* in having a well-developed coronoid process of the mandible, the presence of i1, a long metastyle on M1-2 and a weak paracone fold on M1-2.

DIAGNOSIS DISCUSSION. — Belyaeva (1971) and Lucas *et al.* (1996) mentioned the presence of a third loph on P4 in *Zaisanamynodon borisovi* and Lucas (2006) observed this characteristic in *Zaisanamynodon protheroi*. He considered this feature as a distinct trait of *Zaisanamynodon* from other genera of Metamynodontini, to which *Zaisanamynodon* formerly belonged. In fact, this character can be used to distinguish *Zaisanamynodon* from all genera of Amynodontidae.

Zaisanamynodon borisovi Belyaeva, 1971

(Figs 3; 4; Table 2)

Zaisanamynodon borisovi Belyaeva, 1971: 43.

TYPE MATERIAL. — Holotype ANPIN 2761/1-22, incomplete skull, lower jaw, and part of the postcranial skeleton, including most of the cervical vertebrae and forelimbs (Belyaeva 1971).

REFERRED MATERIAL. — ZSN-KKS-28-IPB, fragmentary skull with P2-M3 in connection with a fragmentary mandible with p4-m3. MJSN.2020.008.01 and MJSN.2020.008.02 are 3D-printed copies of this skull and mandible, respectively.

TYPE LOCALITY AND HORIZON. — Kiin Kerish locality (48°07'52.2"N, 84°28'52.3"E), north-west of Kiin Kerish Mountain, Kazakhstan. Lower Aksyir Svita, Ergilian ALMA (36.5–33.9 Ma) (i.e., late Eocene) (Borisov 1963; Belyaeva 1971; Russell & Zhai 1987; Lucas & Emry 1996; Lucas *et al.* 1996; Emry *et al.* 1998; Vandenberghe *et al.* 2012).

EMENDED DIAGNOSIS. — Differs from *Zaisanamynodon protheroi* in having a relatively short rostrum (about 12% of skull length), an anterior margin of the orbit above M1, incisors relatively large (especially I3/i3), a P2 less complex without anterior and posterior crests connected to the metaloph, a weak paracone fold on M3, lower canine relatively slender and curved, p3 more molariform, and a slight labial groove (cleft) between trigonid and talonid on lower molars.

DIAGNOSIS DISCUSSION. — In the revised diagnosis of *Z. borisovi* in Lucas (2006), the “lack of a complete cingulum” on P2-4 is considered as a character to distinguish *Z. borisovi* from *Zaisanamynodon protheroi*. However, in the original diagnosis of *Zaisanamynodon borisovi*, Belyaeva (1971) mentioned the presence of a well-developed anteroposterior and lingual collar (i.e., cingulum) and a weak labial collar (i.e., cingulum) on the upper premolars. In the description of Chinese specimens of *Z. borisovi*, Lucas *et al.* (1996) indicated the presence of a “complete lingual cingulum” on P2-3, and a “postero-lingual cingulum” on P4, which has been confirmed after direct observation of the specimen AMNH.26034. This feature is also observed on the studied material (ZSN-KKS-28-IPB). Therefore, the lingual cingulum on P2-4 can no longer be considered as a diagnostic character to distinguish *Z. protheroi* from *Z. borisovi*.

DESCRIPTION

Skull and mandible

The skull ZSN-KKS-28-IPB (Fig. 3A, B) is incomplete, deformed and some parts are covered by matrix. The maxilla is incomplete, and only the left anterior part of the jugal is still preserved. The anterior margin of the orbit is above

TABLE 1. — List of perissodactyl taxa (Rhinocerotoidea Owen, 1845 plus *Tapirus terrestris* (Linnaeus, 1758)) included in the phylogenetic analysis and their sources of coding.

Terminal	Sources of character coding		
	Direct observations	References	
<i>Aceratherium incisivum</i> Kaup, 1832	—	Antoine et al. (2010); Tissier et al. (2018)	
<i>Allacerops turgaica</i> (Borissiak, 1918)	—	Tissier et al. (2018)	
<i>Amynodon advenus</i> (Marsh, 1875)	—	Tissier et al. (2018)	
<i>Amynodontopsis bodei</i> Stock, 1939	—	Tissier et al. (2018)	
<i>Amynodontopsis jiyuanensis</i> Wang X.-Y., Wang Y.-Q., Zhang R., Zhang Z.-H., Liu & Ren, 2020	—	Wang et al. (2020)	
<i>Cadurcodon ardynensis</i> (Osborn, 1923)	—	Tissier et al. (2018)	
<i>Cadurcodon bahoensis</i> Xu, 1965	—	Tissier et al. (2018)	
<i>Cadurcodon kazakademius</i> Biryukov, 1961	—	Tissier et al. (2018)	
<i>Cadurcodon maomingensis</i> Averianov, Danilov, Jin & Wang, 2016	—	Tissier et al. (2018)	
<i>Cadurcotherium cayluxi</i> Gervais, 1873	—	Collection « Le Garouillas » in De Bonis (1995) and Ménouret (2018)	
<i>Cadurcotherium minum</i> Filhol, 1880	—	Ménouret (2018)	
<i>Eggysodon osborni</i> (Schlosser, 1902)	—	Tissier et al. (2018)	
<i>Hyracetus eximius</i> Leidy, 1871	—	Antoine et al. (2010)	
<i>Hyracodon nebrascensis</i> Leidy, 1850	—	Tissier et al. (2018)	
ZSN-KKS-28-IPB	IPB, MJSN	—	
<i>Megalamynodon regalis</i> Scott, 1945	—	Tissier et al. (2018)	
<i>Metamynodon planifrons</i> Scott & Osborn, 1887	—	Tissier et al. (2018)	
“Pappaceras” <i>meiomenus</i> Wang H.-B., Bai, Meng & Wang Y.-Q., 2016	—	Tissier et al. (2018)	
<i>Paraceratherium bugtiense</i> (Pilgrim, 1908)	—	Tissier et al. (2018)	
<i>Paraceratherium transouralicum</i> (Pavlova, 1922)	—	Tissier et al. (2018)	
<i>Paramynodon birmanicus</i> (Pilgrim & Cotter, 1916)	—	Tissier et al. (2018)	
<i>Ronzotherium filholi</i> (Osborn, 1900)	—	Antoine et al. (2010); Tissier et al. (2018)	
<i>Rostramynodon grangeri</i> Wall & Manning, 1986	—	Tissier et al. (2018)	
<i>Sellamynodon zimborensis</i> (Codrea & Suraru, 1989)	—	Tissier et al. (2018)	
<i>Sharamynodon mongoliensis</i> (Osborn, 1936)	—	Tissier et al. (2018)	
<i>Tapirus terrestris</i> (Von Linnaeus, 1758)	—	Antoine et al. (2010); Tissier et al. (2018)	
<i>Teletaceras radinskyi</i> Hanson, 1989	—	Tissier et al. (2018)	
<i>Trigonias osborni</i> Lucas, 1900	—	Antoine et al. (2010)	
UNISTRA.2015.0.1106	UNISTRA	—	
<i>Urtinotherium intermedium</i> (Chiu, 1962)	—	Tissier et al. (2018)	
<i>Zaisanamynodon borisovi</i> Belyaeva, 1971	—	Tissier et al. (2018)	
<i>Zaisanamynodon protheroi</i> Lucas, 2006	—	Tissier et al. (2018)	

M1. The zygomatic process progressively diverges from the maxilla. It starts above the M2 and separates from it above the M3. The mandible ZSN-KKS-28-IPB (Fig. 4A, B) is incomplete; the most anterior part is absent. The corpus mandibulae has a straight ventral profile. Only the anterior part of the ramus is present, and it is vertical. The dental formula of the specimen is I 1/1, C 1/1, P 3/2? M 3/3. The upper and lower anterior dentition are not preserved. The dental wear of the cheek teeth is moderate, the crown height is low, and the enamel is wrinkled and corrugated. The right P2 is very worn. The left P2 is not preserved and the left M3 is covered by matrix. There is no cement, crochet or antecrochet. The left p3 is not preserved but the roots of the right p3 can be observed in occlusal view.

Upper cheek teeth (Fig. 3C-G)

The upper premolars are not molarized and are very short compared to the molars (*sensu* Antoine 2002), with a LP3-4/LM1-3 ratio ≤ 0.42 . Premolars have a labial and lingual cingulum. The lingual cingulum is strong and continuous. The postfossette is wide. The P2 is very small. It bears a single labial cusp and probably had a single lingual one.

The labial cingulum is continuous. On P3-4, the protocone and the hypocone are fused into a single lingual cusp. The protocone is not constricted. The metaloph is directed posterolingually. The paracone fold is very strong, forming a well-developed vertical ridge. On P3, the protoloph is not joined to the ectoloph, whereas they are joined on P4. The hypocone and the metacone of P4 are separated, whereas they are joined for P3. There is a crista on P3 and on the left P4. There is a shallow groove separating the paracone and the metacone on the ectoloph of P4. The metaloph of P4 is very short and weak. P4 has a third loph (Fig. 3F), posterior to the metaloph and closing the postfossette. This third loph is thin, low, and discontinuous.

The upper molars have a π shape. They have a weak labial cingulum; a weak lingual cingulum is present in anterior and/or posterior parts of M2 and posterior part of M3 whereas lingual cingulum is lacking on M1. Therefore, character 109 (1) and character 114 (2) in the matrix are scored as “usually present” and “usually absent”, respectively (*sensu* Antoine 2002). There are no crista and cristella. The protocone is widened. The metaloph is short, continuous, and its width decreases between M1-3. The ectoloph is very long, straight,

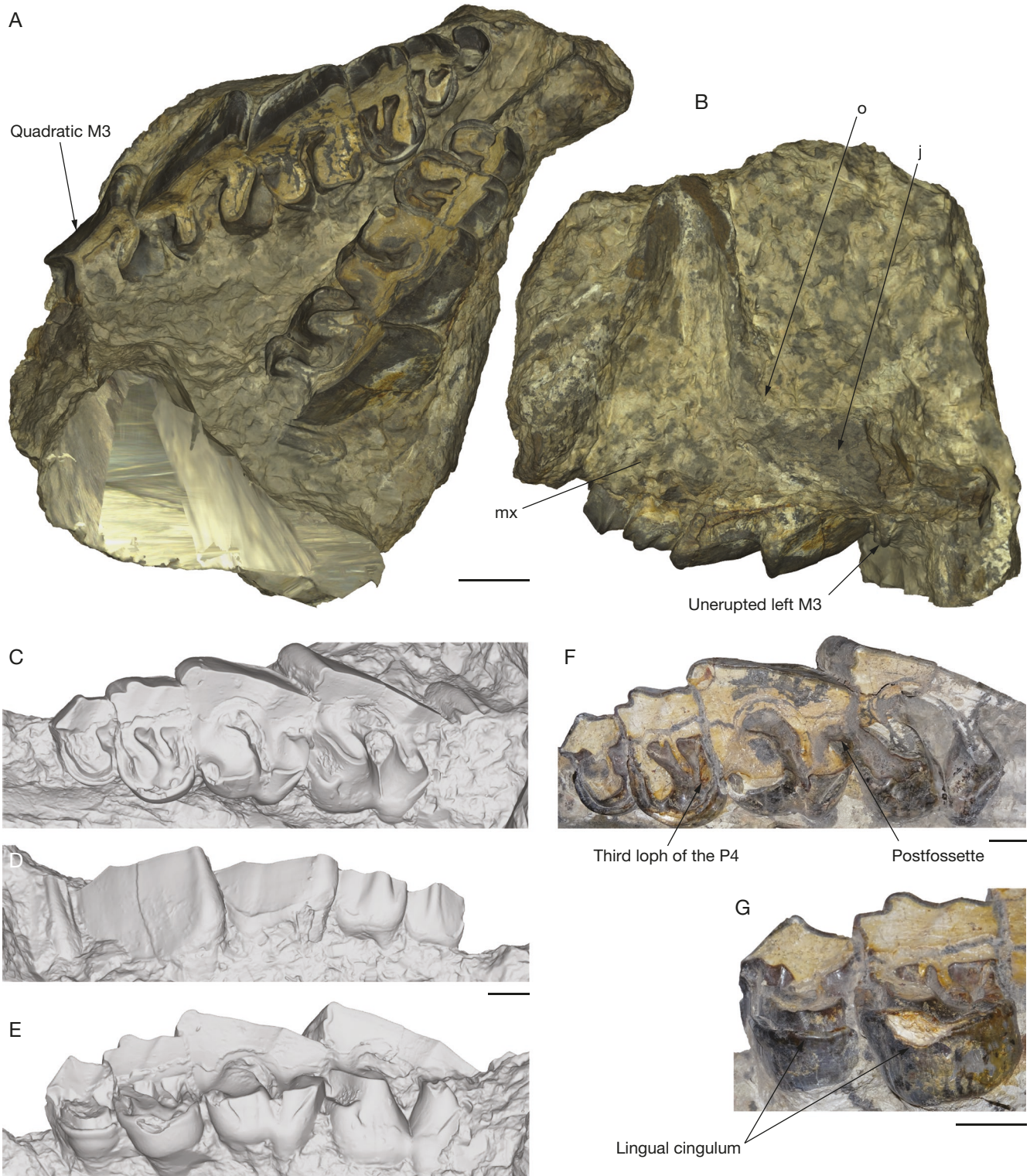


Fig. 3. — Skull and upper cheek teeth of the amynodontid rhinocerotoid *Zaisanamynodon borisovi* Belyaeva, 1971, ZSN-KKS-28-IPB, Kiin Kerish, Kazakhstan, late Eocene: A, B, skull, three-dimensional model with texture, occlusal (A) and left lateral views (B); C–E, close-up of the left cheek teeth series, P4–M2(3), three-dimensional model, occlusal (C), lateral (D), lingual (E) views; F, close-up of the left cheek teeth series, P4–M2, occlusal view; G, close-up of the left P4–M1, lingual view. Abbreviations: j, jugal; mx, maxilla; o, orbit. Scale bars: A, B, 5 cm; C–G, 2 cm.

and smooth. The fold of the paracone is weak, and the parastyle is reduced. There is a postfossette on each molar. The metastyle on M1–2 is long. The M1–2 have a continuous posterior cin-

gulum. The M3 has a quadrangular shape. Its protoloph and metaloph are oblique to its ectoloph. Its metastyle is directed posterolingually. The ectoloph is concave labially.

TABLE 2. — Measurements (in mm) of the dentition of the amynodontid rhinocerotoid *Zaisanamynodon borisovi* Belyaeva, 1971 ZSN-KKS-28-IPB. The width measurements of P4-M3 are presented as follows: anterior/posterior orientation of the teeth. The measurements are in brackets when they are uncertain.

Tooth	Length		Width		Height	
	Left	Right	Left	Right	Left	Right
P2	—	24.5	—	(25.0)	—	28.0
P3	32.5	31.0	46.0	44.0	31.0	32.5
P4	38.5	38.0	61.0 / 56.0	60.0 / 50.0	32.5	32.0
M1	67.0	70.0	68.0 / 67.0	68.0 / 65.0	35.0	39.0
M2	81.0	81.0	69.0 / 62.0	60.0 / 40.0	54.0	57.0
M3	—	82.5	—	47.0 / —	—	57.0
p4	37.0	39.0	30.5	31	35.0	38.0
m1	57.0	56.0	36.5	38.5	38.0	39.0
m2	75.0	74.5	45.0	47.0	49.5	47.0
m3	82.0	80.5	40.0	39.5	50.0	51.0

Lower cheek teeth (Fig. 4C-H)

The p4-m3 series have a continuous labial cingulum. The lingual cingulum is only interrupted below the hypoconid. The trigonid is obtuse and is smaller than the talonid. The trigonid and talonid are open on the lingual side. The talonid is equal to the trigonid on the p4-m1, whereas the talonid is longer than the trigonid on the m2-3. The metaconid and entoconid are not constricted. The ectolophid is completely smooth (no labial groove), except on the p4, which has very shallow ectolophid and paralophid grooves. The lingual opening of the posterior valley on the p4 is U-shaped. The lower molar series are long. They bear an oblique hypolophid.

Body mass

The body mass of ZSN-KKS-28-IPB was estimated to be around 4.1 tons with the regression equations of perissodactyls and ungulates of Legendre (1989) based on occlusal surface of m1 (Table 2; Appendix 3). The body mass was also estimated to be around 5.7 tons with the regression equations of Rhinocerotidae of Fortelius & Kappelman (1993), and 4.5 tons with the equations for all ungulates. They are based on the lengths of M2, M3 and the total upper tooth row (Table 2; Appendix 3). In most cases, our estimations are higher than those of Averianov *et al.* (2016) for *Zaisanamynodon borisovi* (“2442 ± 257 kg” see Averianov *et al.* (2016): supplemental table 2) with regression equation for generalized ungulates of Legendre (1989), except for the TRLU estimate (2.1 tons). This can be explained by the very large dimensions of the cheek teeth of the referred specimen as well as by the much bigger size of M2 and M3 (which are not used by Averianov *et al.* 2016), compared to the m1.

Furthermore, the body mass estimation obtained through the Rhinocerotidae equations of Fortelius & Kappelman (1993) based on M2 and M3 may also be extremely overestimated due to the difference of morphology of the teeth of Amynodontidae compared with Rhinocerotidae. Indeed, in Amynodontidae, the M2 and M3 tend to be much larger than all other cheek teeth, which is not the case in Rhinocerotidae. In addition, Amynodontidae retain a metastyle on M3, leading to a quadrangular shape (and thus bigger

length), whereas Rhinocerotidae have a triangular M3, without metastyle but an ectometaloph instead. Thus, these values should not be taken at face value but only be used for comparison if one uses the same method, since there are currently none that is specifically made for the rather peculiar Amynodontidae morphology.

Interestingly, the dimensions of the M2 and M3 of this specimen are comparable to those of the largest land-mammal that ever existed: *Paraceratherium* (= *Indricotherium*). For example, the length of M2 and M3 of *Paraceratherium bugtiense* is around 74 to 96 mm (Fortelius & Kappelman 1993), while our specimen measures 81 and 82 mm respectively. This explains the enormous body mass retrieved by our estimations. However, these estimations can be nuanced by the much shorter upper tooth row length (284 mm for ZSN-KKS-28-IPB against 400 mm for “*Indricotherium transouralicum*”), which is explained by the typical premolar reduction of the Amynodontidae. Therefore, *Zaisanamynodon borisovi* may still have been one of the largest Amynodontidae, but not as large as *Paraceratherium*.

REMARKS

ZSN-KKS-28-IPB can be referred to Rhinocerotoidea based on the π shape of upper molars (Wall 1989). An attribution of ZSN-KKS-28-IPB to Amynodontidae is reliable based on the reduced dental formula, with the absence of the P1/p1-2, which is a derived character typical of Amynodontidae (Wall 1989; Tissier *et al.* 2018). ZSN-KKS-28-IPB shares other diagnostic characters of the Amynodontidae: the absence of the crochet; antecrochet; crista; the reduced parastyle on the upper molars; the quadratic M3 with a large metastyle and the elongated lower molars (Wall 1989; Tissier *et al.* 2018). Therefore, an attribution to Rhinocerotidae, Eggysodontidae, “Hyracodontidae” or Paraceratheriidae can be excluded.

According to our phylogenetic analysis, ZSN-KKS-28-IPB shares two diagnostic characters with Cadurcodontini: a talonid on m3 longer than the trigonid and the constant presence of labial cingulum on upper premolars. It also shares the absence of labial groove separating the trigonid and talonid on lower molars (Averianov *et al.* 2016).

Within Cadurcodontini, ZSN-KKS-28-IPB differs from *Cadurcotherium* in the absence of cement on cheek teeth, an oblique hypolophid on lower molars, and a long metastyle on M1-2. ZSN-KKS-28-IPB differs from *Amynodontopsis* in the presence of a postfossette on M1. ZSN-KKS-28-IPB differs from *Cadurcodon* in having a long metastyle on M1-2 and a weak paracone fold on M1-M2.

ZSN-KKS-28-IPB can be referred to *Zaisanamynodon* by the presence of a third posterior loph on P4, which is a diagnostic character of the genus (Lucas 2006). Belyaeva (1971), Lucas *et al.* (1996) and Lucas (2006) provided detailed descriptions, illustrations, and measurements of *Zaisanamynodon borisovi* and *Zaisanamynodon protheroi*. Following our emended diagnosis of *Z. borisovi*, ZSN-KKS-28-IPB shares a single diagnostic character of *Z. borisovi*: the anterior margin of the orbit above M1. However, ZSN-KKS-28-IPB differs from it by the absence of slight labial groove (cleft) between trigonid

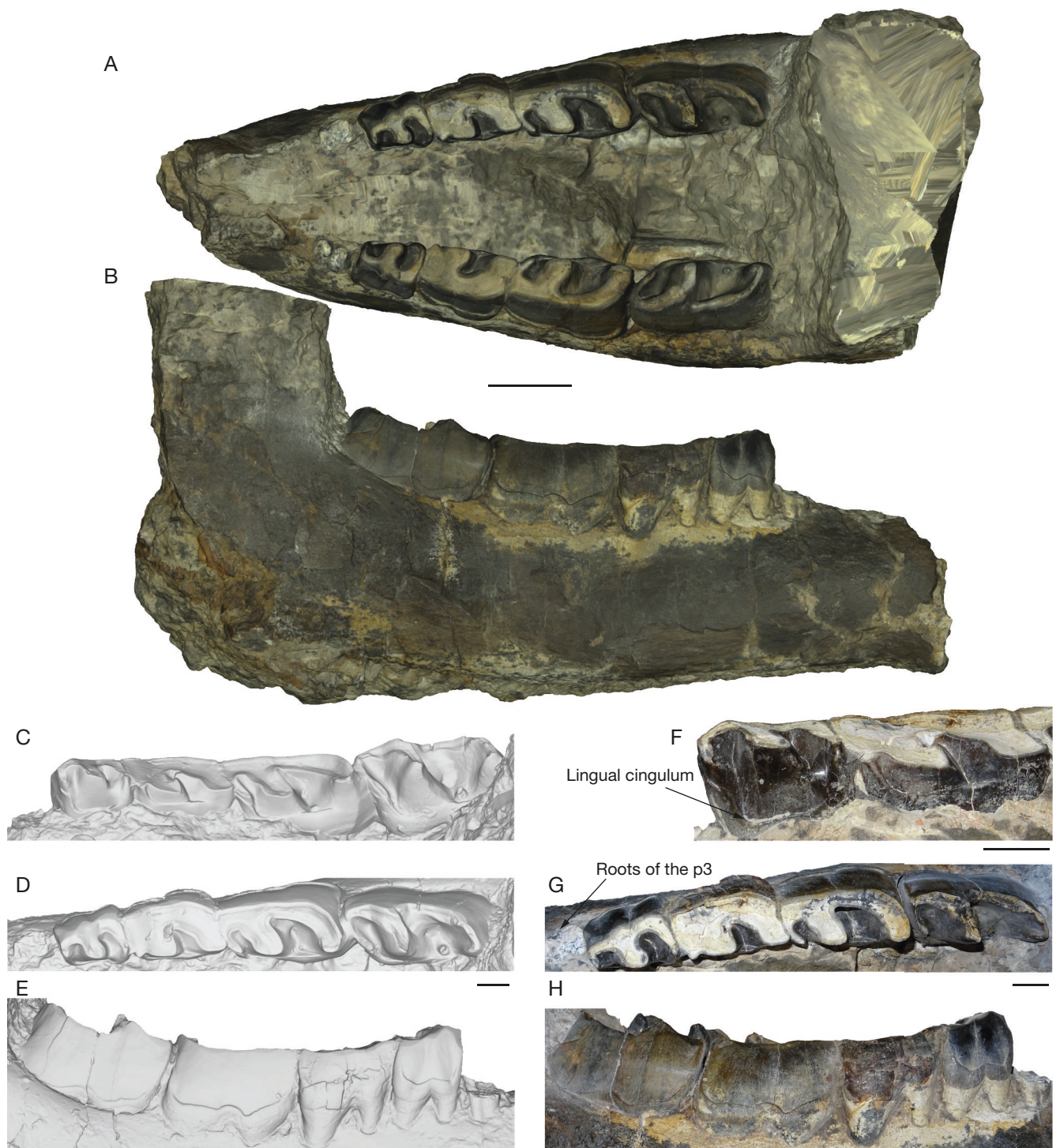


FIG. 4. — Mandible and lower cheek teeth of the amynodontid rhinocerotoid *Zaisanamynodon borisovi*, 1971 ZSN-KKS-28-IPB, Kii Kerish, Kazakhstan, late Eocene: **A, B**, mandible, three-dimensional model with texture, occlusal (**A**), right lateral (**B**) views; **C-E**, close-up of the right cheek teeth series, p3-M3, three-dimensional model, lingual (**C**), occlusal (**D**), lateral (**E**) views; **F**, close-up of the right p4-m1, lingual view; **G, H**, close-up of the right cheek teeth series, p3-M3, occlusal (**G**), lateral (**H**) views. Scale bars: A, B, 5 cm; C-H, 2 cm.

and talonid on lower molars, as in *Z. protheroi*. According to Lucas (2006), the complexity of the P2 and the presence of an “anterior and posterior crests connected to metaloph” are considered as differential diagnostic characters of the two species of *Zaisanamynodon*. This feature cannot be observed on ZSN-KKS-28-IPB because the right P2 is very worn and

the left one is missing. For this reason, we cannot use this character to exclude an attribution to *Z. protheroi* (Lucas 2006). In addition, the incisors, canines and p3, which also bear diagnostic characters to differentiate *Z. borisovi* from *Z. protheroi*, are not preserved. However, the paracone fold on M3 is weak in ZSN-KKS-28-IPB as in *Z. borisovi*, and

TABLE 3. — Measurements (in mm) of the upper cheek teeth and skull of the amynodontid rhinocerotoid *Metamynodon planifrons* Scott & Osborn, 1887, UNISTRA.2015.0.1106. The width measurements of M1-3 are presented as follows: anterior/posterior orientation of the teeth. The measurements are in brackets when they are uncertain.

Tooth	Length		Width		Height	
	Left	Right	Left	Right	Left	Right
P2	15.0	15.0	18.5	18.0	—	—
P3	17.0	19.0	27.5	29.0	—	—
P4	24.5	24.0	40.0	43.0	—	—
M1	35.5	33.5	56.5/48.0	56.0/50.0	—	—
M2	50.5	50.0	63.5/50.5	61.0/48.5	(15.0)	(14.0)
M3	60.0	60.5	55.0/32.5	55.5/33.0	(14.5)	(14.0)
Skull	—	—	—	—	—	—
Premaxilla to orbit	160	—	—	—	—	—
Premaxilla to occipital	555	—	—	—	—	—

contrary to *Z. protheroi* (Belyaeva 1971; Lucas *et al.* 1996; Lucas 2006), which is the only character that supports the assignment of this specimen to *Z. borisovi* in our phylogenetic analysis. Therefore, based on these anatomical comparisons of ZSN-KKS-28-IPB with Belyaeva (1971), Lucas *et al.* (1996) and Lucas (2006), ZSN-KKS-28-IPB can only be tentatively assigned to *Zaisanamynodon borisovi*.

Moreover, two species of Amynodontidae, *Cadurcodon ardynensis* (Osborn, 1923) and *Zaisanamynodon borisovi* are known from the Zaysan basin in north-west Kazakhstan (Lucas & Emry 1996; Emry *et al.* 1998). *Cadurcodon ardynensis* is known from the Kusto Svita at Kiin Kerish and from the Buran Svita at Kalmakpay Mountain (Lucas & Emry 1996; Emry *et al.* 1998). The presence of a third loph on P4 excludes an attribution of ZSN-KKS-28-IPB to *Cadurcodon*. The holotype of *Zaisanamynodon borisovi* (ANPIN 2761/1-22; Belyaeva, 1971) and ZSN-KKS-28-IPB both come from the Lower Aksyir Svita at Kiin Kerish. Thus, this supports our identification of ZSN-KKS-28-IPB as *Zaisanamynodon borisovi*.

Tribe METAMYNODONTINI Kretzoi, 1942

Genus *Metamynodon* Scott & Osborn, 1887

Metamynodon Scott & Osborn, 1887: 165.

TYPE SPECIES. — *Metamynodon planifrons* Scott & Osborn, 1887.

INCLUDED SPECIES. — According to literature *Metamynodon chadronensis* Wood, 1937, *Metamynodon mckinneyi* Wilson & Schiebout, 1981 are included in *Metamynodon*. However, some revision work of both species seems to be needed to assess their validity. Indeed, diagnostic characters used to describe *M. chadronensis* Wood, 1937 and *M. mckinneyi* Wilson & Schiebout, 1981 are not specific enough to distinguish them from the type species.

EMENDED DIAGNOSIS. — Within Metamynodontini, *Metamynodon* differs from other genera (*Paramynodon* Matthew, 1829, *Megalamynodon* Wood, 1945, and *Sellamynodon* Tissier, Becker, Codrea, Costeur, Fărcaș, Solomon, Venczel & Maridet, 2018) in having large and tusk-like canines, high-crowned cheek teeth, the

labially confluent trigonid and talonid, the premaxilla and the nasal reduced but still contacting each other along the border of external nares, a very large and massive zygomatic arch, a massive lower jaw (Wall 1989). *Metamynodon* differs from *Sellamynodon* in having a high zygomatic arch, a flat dorsal profile of the skull, the presence of a sagittal crest, a circular magnum foramen and m3 talonid equal or smaller than trigonid. *Metamynodon* differs from *Megalamynodon* in having a well-developed paroccipital process and strong upper canines. *Metamynodon* differs from *Paramynodon* in having a protoloph on P2, an upper postcanine diastema shorter than the length of upper premolars and the orbit positioned higher on the skull.

REMARK

Diagnosis same as for the type species.

Metamynodon planifrons Scott & Osborn, 1887 (Figs 5; 6 ; Table 3)

Metamynodon rex Troxell, 1921: 24.

Metamynodon planifrons — Scott & Osborn 1887: 165.

TYPE MATERIAL. — Holotype. VPM-9157, skull and anterior part of the left mandible (Scott & Osborn 1887; see online the database of the Zoological Collections of the Museum of Comparative Zoology - Harvard University).

REFERRED MATERIAL. — UNISTRA.2015.0.1106, skull with right C1 and P2-M3.

TYPE LOCALITY AND HORIZON. — Big Badlands, South Dakota, United States. White River Group, Brule Formation, early Oligocene (Scott & Osborn 1887; Scott 1941; Benton *et al.* 2015).

DESCRIPTION

Skull

The skull UNISTRA.2015.0.1106 is incomplete (Fig. 5). The anterior surface of the nasal is damaged and its extremity lacking. The right orbit is filled with matrix. The skull is brachycephalic (*sensu* Antoine 2002), with a maximum zygomatic width/nasal-occipital length ratio >0.50. The preorbital region constitutes less than 30% of the skull. There are no rugosities suggesting the presence of a horn.

In lateral view (Fig. 5A, B), the dorsal profile of the skull is flat. The tooth row extends beyond the middle of the skull. The premaxilla and the nasal contact each other along the border of external nares. The nasal incision is in front of the P2. The nasal, frontal and maxilla contact each other. There is a reduced and deep preorbital fossa. The anterior border of the orbit is above P4-M1. The orbit is relatively high on the skull. The anterior base of the zygomatic process of the maxilla is low. The position of the zygomatic arch on the skull is high. On the squamosal, a posterior groove on the zygomatic process is present. Both squamosal and frontal have a postorbital process. The squamosal area between the temporal and nuchal crests is flat. The external acoustic pseudomeatus is closed. The posterior margin of the pterygoid is nearly horizontal. The occipital side inclines posteriorly. A poorly developed nuchal tubercle (or occipital protuberance) on the occipital is present.

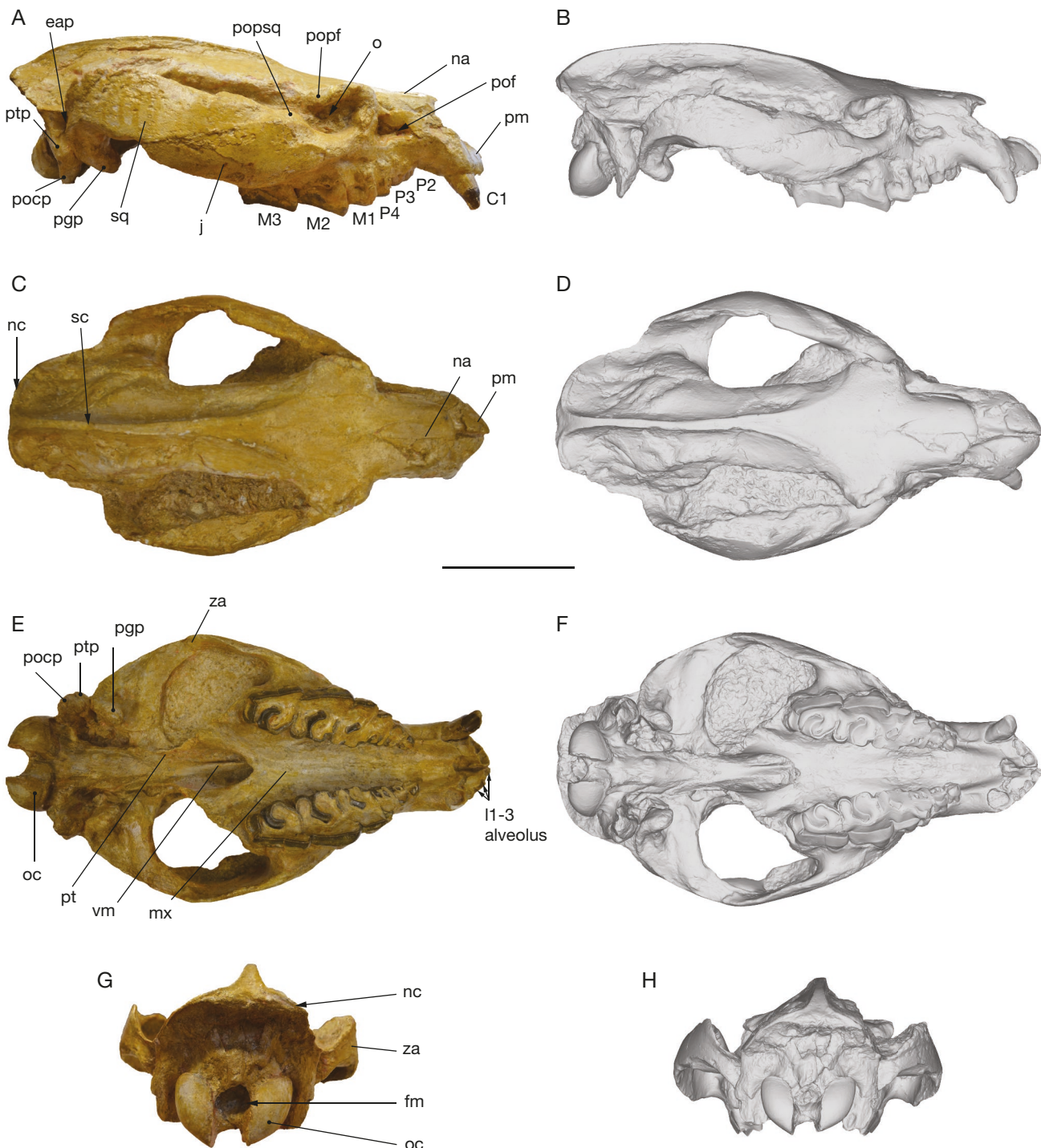


Fig. 5. — Skull of the amynodontid rhinocerotoid *Metamynodon planifrons* Scott & Osborn, 1887, UNISTRA.2015.0.1106, Big Badlands, South Dakota, United States, early Oligocene: **A**, right lateral view; **B**, three-dimensional model, right lateral view; **C**, dorsal view; **D**, three-dimensional model, dorsal view; **E**, ventral view; **F**, three-dimensional model, ventral view; **G**, occipital view; **H**, three-dimensional model, occipital view. Abbreviations: **eap**, external auditory pseudomeatus; **fm**, foramen magnum; **j**, jugal; **mx**, maxilla; **na**, nasal; **nc**, nuchal crest; **o**, orbit; **oc**, occipital condyle; **ppg**, postgenoid process; **pm**, premaxilla; **pocp**, paraoccipital process; **pof**, postorbital fossa; **popf**, postorbital process of the frontal; **popsq**, postorbital process of the squamosal; **pt**, pterygoid; **ptp**, posttympanic process; **sc**, sagittal crest; **sq**, squamosal; **vm**, vomer; **za**, zygomatic arch. Scale bar: 10 cm.

In dorsal view (Fig. 5C, D), the zygomatic arches are wide and massive. The zygomatic index (maximum width at the zygomatic/maximum width at the frontals) is 1.55 (*sensu* Antoine 2002). The sagittal crest is strong. The external occipital protuberance is straight.

In ventral view (Fig. 5E, F), the zygomatic arches are complete and diverge abruptly from the maxilla. It starts above the M2 and separates above the M3. The vomer is acute. The post-glenoid apophysis (= process) is flat. The posttympanic process is fused to the postglenoid process. The posttympanic

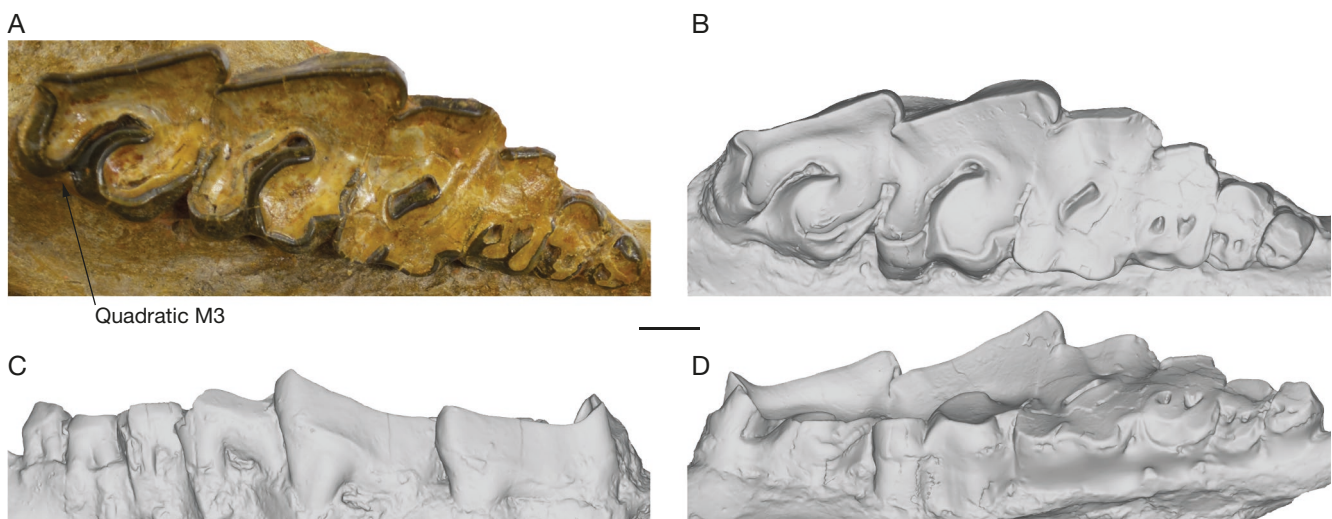


FIG. 6. — Upper cheek teeth of the amynodontid rhinocerotoid *Metamynodon planifrons* Scott & Osborn, 1887, UNISTRA.2015.0.1106, Big Badlands, South Dakota, United States, early Oligocene: **A**, close-up of the right cheek teeth series, P2-M3, occlusal view; **B-D**, close-up of the right cheek teeth series, P2-M3, three-dimensional model, occlusal (**B**), lateral (**C**) and lingual views (**D**). Scale bar: 2 cm.

process is poorly developed but the paroccipital process is developed and fused together.

In occipital view (Fig. 5G, H), the foramen magnum is circular. The dental formula is I 3/?; C 1/?; P 3/?; M 3/? . The alveoli of the incisors and the left canine can be observed in occlusal view. The right canine is in place, strong and cylindrical. The diastema between the canines and premolars is short. The series of premolars and molars are complete but worn. The premolar series are very short compared to the molar series (*sensu* Antoine 2002), with a LP3-4/LM1-3 ratio ≤ 0.42 . There is no crochet and no antecrochet on the upper cheek teeth.

Upper cheek teeth (Fig. 6)

The P3 is submolariform and the P4 is semimolariform (*sensu* Heissig 1969). The protocone and hypocone are connected by a lingual bridge. The premolars have no labial cingulum, and their lingual cingulum is continuous. The postfossette is wide. The metaloph is transverse. On P2, the protoloph is present and does not join to the ectoloph. The hypocone and protocone of P2 are fused. On P3-4, the protoloph is fused to the ectoloph. The hypocone and the metacone are linked. The P4 has a crista.

The upper molars have a π form (Fig. 6A). They have neither lingual nor labial cingula. There is no constriction of the protocone. The parastyle is reduced. There is no crista and cristella. On M1-2, the protocone and hypocone are fused. There is no paracone fold. The metaloph is continuous and long, the metacone fold is absent. The metastyle is short. The posterior part of the ectoloph is straight. The M3 has quadrangular shape. The protoloph is transverse, the ectoloph and metaloph are distinct. The paracone fold is weak. The metastyle is directed posterolingually.

Body mass

The body mass of UNISTRA.2015.0.1106 was estimated to be around 1.3 and 1.2 tons with the regression equations for

the Rhinocerotidae and all Ungulates respectively (Fortelius & Kappelman 1993). They are based on several measurements, including M2 and M3 lengths, basicondylar length, or zygomatic width (Table 3; Appendix 3).

Our estimations are lower than those of Averianov *et al.* (2016) for *Metamynodon planifrons* (*c.* “1794 kg”, see Averianov *et al.* (2016): supplemental table 2) based on the occlusal surface of m1, with the regression equation for generalized ungulates of Legendre (1989). This method can't be applied to UNISTRA.2015.0.1106 because it is a skull, without mandible. As a comparison, similar results to ours were obtained estimating the body mass of VPM-9157 (Scott & Osborn (1887); holotype of *M. planifrons*), with the same equation, based on M3 length, basicondylar length, and zygomatic width (Table 3; Appendix 3). The body mass of VPM-9157 was estimated to be around 1.5 and 1.3 tons with the regression equations for the Rhinocerotidae and all Ungulates respectively (Fortelius & Kappelman 1993).

Despite this, our results are certainly over-estimated because the same problems with these methods explained earlier for *Zaysanamynodon* also apply to this genus (i.e., M2 and M3 much larger than all other cheek teeth in Amynodontidae, and retention of a metastyle on M3).

REMARKS

UNISTRA.2015.0.1106 can be referred to Rhinocerotoidea based on the π -shape form of upper molars (Wall 1989). An attribution of UNISTRA.2015.0.1106 to Amynodontidae is reliable based on the reduced upper dental formula, with the absence of P1, which is a derived character typical of Amynodontidae (Wall 1989; Tissier *et al.* 2018). UNISTRA.2015.0.1106 shares other diagnostic characters of the Amynodontidae: the absence of the crochet, antecrochet and crista; the reduced parastyle on the upper molars; the quadratic M3 with a large metastyle; the absence of horn; the presence of a preorbital fossa and a large sagittal crest

(Wall 1989; Tissier *et al.* 2018). Therefore, an attribution to Rhinocerotidae, Eggysodontidae, “Hyracodontidae” or Paraceratheriidae can be excluded.

UNISTRA.2015.0.1106 shares diagnostic characters of the Metamynodontini: the presence of the frontal-maxilla contact, a brachycephalic skull, an orbit positioned high on the skull, a reduced preorbital fossa and a wide, massive zygomatic arch (Wall 1989).

Within Metamynodontini, UNISTRA.2015.0.1106 differs from *Sellamynodon* in having: a high zygomatic arch; a flat dorsal profile of the skull; the presence of a sagittal crest; a circular foramen magnum. UNISTRA.2015.0.1106 differs from *Megalamynodon* in having a well-developed paroccipital process. UNISTRA.2015.0.1106 differs from *Paramynodon* in having a protoloph on P2, an upper postcanine diastema shorter than the length of the upper premolars and the orbit positioned higher on the skull. UNISTRA.2015.0.1106 can be referred to *Metamynodon* by the presence of large and tusk-like canines, the premaxilla and the nasal reduced but still contact each other along border of external nares, a very large and massive zygomatic arch (Wall 1989).

Three species of *Metamynodon* are considered as valid: *Metamynodon chadronensis*, *Metamynodon mckinneyi* and *Metamynodon planifrons*. *Metamynodon chadronensis* is known from fragmented skulls, mandibles, and isolated teeth (Wood 1937; Wilson & Schiebout 1981). *Metamynodon mckinneyi* is only known from a mandible while our new material UNISTRA.2015.0.1106 to identify is a skull, so no direct comparison was possible. The holotype of *M. chadronensis* is also a lower jaw, but some incomplete skulls have been attributed to this species by Wilson & Schiebout (1981). These identifications are mostly based on dental measurements of the lower jaw, which are smaller than *M. planifrons*. However, the dimensions of the upper teeth do not really reflect this smaller dimension and sometimes fit within the observed range of measurements of *M. planifrons* (see Wilson & Schiebout 1981: table 14). Thus, in the absence of a lower jaw and of a clearer distinction between *M. chadronensis* and *M. planifrons*, we refer our specimen to *M. planifrons*, the type species of the genus, as primarily identified by Wood, in Gillet (1960). Furthermore, in our phylogenetic analysis UNISTRA.2015.0.1106 also shares with *M. planifrons* “a low anterior base of the zygomatic process of maxilla”; “an acute vomer”; and “a weak paracone fold on M3”.

RESULTS

Only one most parsimonious tree of 805 steps ($CI = 0.3938$; $RI = 0.4906$) was obtained by using the traditional search of TNT version 1.5 (Fig. 7). The same result was also found with the heuristic search of PAUP* version 4.0a167. The complete list of transformations was obtained with the “tree description” command of PAUP* version 4.0a167 (Appendices 4; 5).

Results concerning the phylogenetic relationships within and between the families of Rhinocerotoidea show a similar topology as Tissier *et al.* (2018), from which we used the

matrix. Rhinocerotidae, Eggysodontidae, Paraceratheriidae and Amynodontidae form monophyletic groups.

RHINOCEROTIDAE

The monophyly of Rhinocerotidae, including *Trigonias osborni* Lucas, 1900, *Aceratherium incisivum* Kaup, 1832 and *Ronzotherium filholi* (Osborn, 1936), is supported by eleven unambiguous synapomorphies: presence of a sagittal crest on the basilar process 44 (1); i2 is tusk-like 79 (1); i3 is absent 81 (1); c1 is absent 82 (1); p2 paralophid is isolated, spur-like 154 (0); semilunate distal border of anterior side is acute 212 (0); magnum posterior tuberosity is long 220 (1); unciform posterior expansion of the pyramidal-facet is usually absent 223 (1); astragalus (Transverse Diameter/Height) ratio = 1 < TD/H < 1.2 252 (1); astragalus (Antero-Posterior Diameter/Height) ratio = 0.65 253 (1); proximal border of the anterior side of the metacarpal III is straight 271 (0). The clade is weakly supported (Bremer index = 1). The species *Hyrachys eximius* Leidy, 1871 is placed as the sister taxon of the Rhinocerotidae.

“HYRACODONTIDAE”

Teletaceras radinskyi Hanson, 1989 is placed as an early-diverging rhinocerotoid and as a sister taxon to the clade including the Eggysodontidae, the Paraceratheriidae and the Amynodontidae. The monophyly of Eggysodontidae is supported by five unambiguous synapomorphies: protocone and hypocone on P2 form a lingual bridge 94 (1); the hypocone is anterior to metacone on P3-4 103 (2); M3 ectoloph and metaloph are fused (ectometaloph) 133 (1); navicular cross section is rectangle 268 (1); lower canines are strong 284 (2). The clade has a Bremer index = 2. Eggysodontidae are sister group of the clade formed by *Hyracodon nebrascensis* Leidy, 1850, Paraceratheriidae and Amynodontidae. *Hyracodon nebrascensis* is a sister taxon to Paraceratheriidae and Amynodontidae. Three unambiguous synapomorphies support the monophyly of Paraceratheriidae: nearly horizontal symphysis 53 (2); M3 ectoloph and metaloph are fused (ectometaloph) 133 (1); atlas axis-facets are transversally concave 187 (2) and it is weakly supported (Bremer index = 1).

AMYNODONTIDAE

“*Pappaceras*” *meiomenus* Wang H.-B., Bai, Meng & Wang Y.-Q., 2016 shares with Amynodontidae seven unambiguous synapomorphies: compared length of the premolar/molar rows < 42 63 (2); P1 in adults is usually present 91 (1); P2 protocone and hypocone are fused 94 (0); P3-4 protocone and hypocone are fused 102 (0); upper molars antecrochet is usually absent 110 (1); upper molars lingual cingulum is usually present 114 (1); M1-2 paracone fold is strong 118 (0).

The monophyly of the Amynodontidae is well supported, with a Bremer index of 4. The monophyly of Amynodontidae (here the smallest clade including *Rostriamynodon grangeri* Wall & Manning, 1986 and *Cadurcodon kazakademius* Biryukov, 1961) is defined by five unambiguous synapomorphies: lacrimal process is absent 8 (1); anterior base of the zygomatic process of the maxilla is high 10 (0); P1 in adults is always absent 91 (2); upper canine is strong 283 (2); upper molars parastyle is reduced 296 (1).

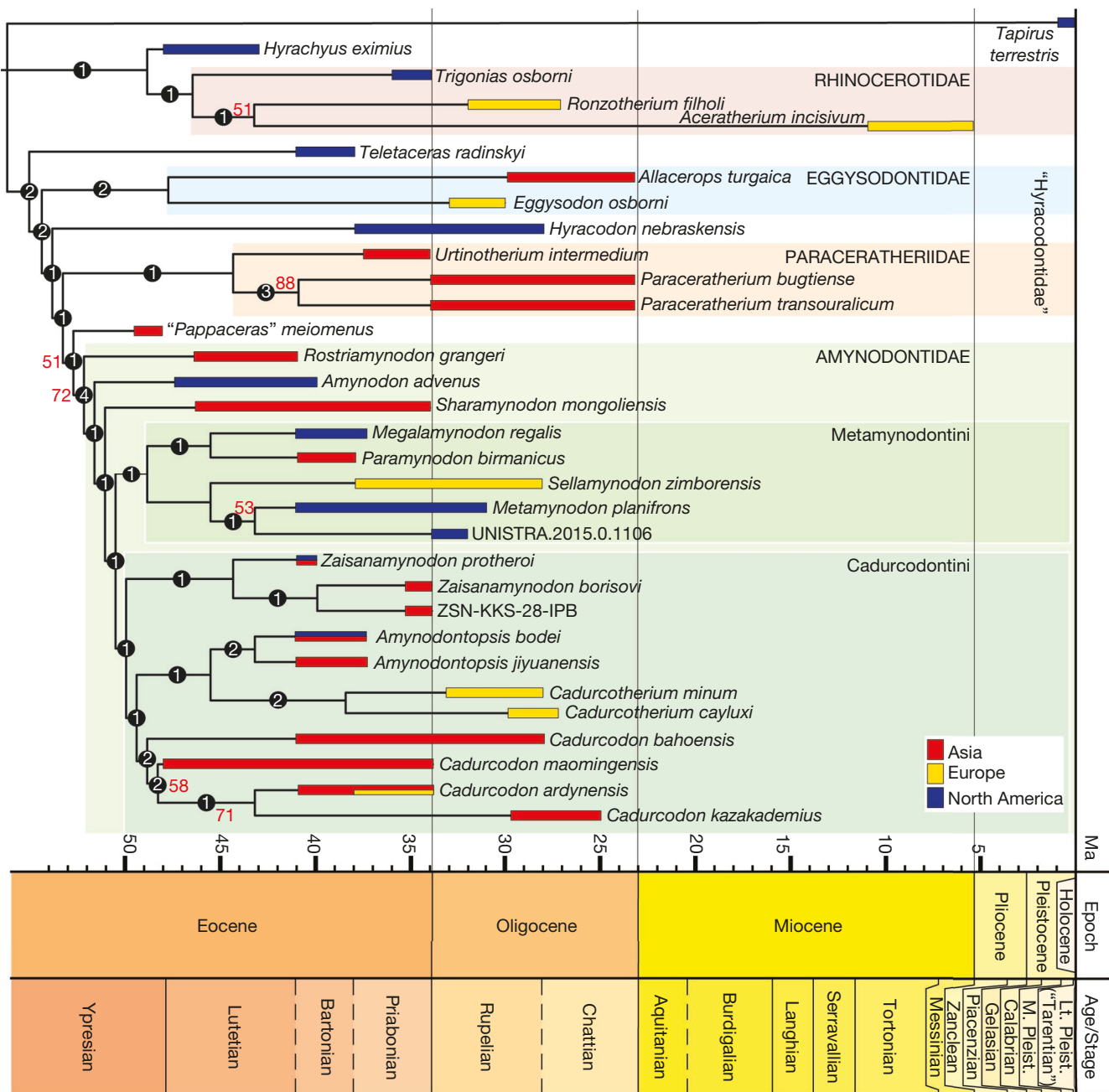


Fig. 7. — Single parsimonious tree of Amynodontidae Scott & Osborn, 1883 within Rhinocerotoidea Owen, 1845, with *Tapirus terrestris* (Linnaeus, 1758) and *Hyrachys eximus* Leidy, 1871 considered as outgroups. Tree length = 806; CI = 0.3933; RI = 0.4912. Numbers at nodes are Bremer support values, **numbers in red** indicate bootstrap values, when greater than 50%. Taxa ages are based on literature as detailed in Table 1. Geological time scale was produced with TSCreator (Ogg 2020).

METAMYNODONTINI

The tribe Metamynodontini is defined by three unambiguous synapomorphies free of homoplasy (Bremer index = 1): the zygomatic arch is high 11 (1); the postglenoid process of squamosal is flat 42 (0); the humerus distal articulation has a deep median constriction (diabolo-shaped) 194 (1). This tribe includes the two clades (*Paramynodon*, *Megalamynodon*) and (*Sellamynodon*, *Metamynodon*).

The clade formed by *Paramynodon* and *Megalamynodon* is supported by two unambiguous synapomorphies (Bremer

index = 1): the zygomatic process progressively diverges from the maxilla 37 (0); I3 has a similar size to I2 293 (1). The clade formed by *Sellamynodon* and *Metamynodon* is supported by a single unambiguous synapomorphy (Bremer index = 1): the external auditory pseudomeatus is closed 18 (2). The specimen UNISTRA.2015.0.1106 is sister group to *Metamynodon planifrons*, which supports its taxonomical identification (Bremer index = 1). *Metamynodon planifrons* (*sensu lato*, = UNISTRA.2015.0.1106 and *M. planifrons*) has three autapomorphies: the anterior base of the zygomatic process

of the maxilla is low 10 (1); the vomer is acute 38 (0); the paracone fold of M3 is absent 289 (1).

CADURCODONTINI

The tribe Cadurcodontini includes *Zaisanamynodon*, *Amynodontopsis*, *Cadurcotherium* and *Cadurcodon*. This clade is defined by five unambiguous synapomorphies (Bremer index = 1): the postglenoid process of squamosal is dihedron 42 (2); the upper premolars labial cingulum is always present 83 (0); the olecranon fossa of the humerus is low 193 (1); the mandibular condylar process is high 287 (0); the talonid of m3 is longer than the trigonid 288 (1).

Zaisanamynodon is placed as a sister group of the clade formed by *Amynodontopsis*, *Cadurcotherium* and *Cadurcodon*. The monophyly of *Zaisanamynodon* is supported by three synapomorphies (Bremer index = 1): the zygomatic process progressively diverges from the maxilla 37 (0); the lingual cingulum of the upper molars is usually absent 114 (2); the third posterior loph is present on P4 298 (1). ZSN-KKS-28-IPB is a sister group of *Zaisanamynodon borisovi*, which supports its identification (Bremer index = 1). *Zaisanamynodon borisovi* (*sensu lato*, = ZSN-KKS-28-IPB and *Z. borisovi*) differs from *Zaisanamynodon protheroi* by a single autapomorphy: the paracone fold of M3 is weak 289 (1). *Zaisanamynodon protheroi* is defined by only one unambiguous autapomorphy: the lingual cingulum of the lower premolars is reduced 148 (0), but five other ambiguous autapomorphies might support the distinction of the two species.

Cadurcotherium and *Amynodontopsis* form a clade supported by three unambiguous synapomorphies (Bremer index = 1): the rostral end of the nasal bones is narrow 24 (0); the mandibular ramus is inclined posteriorly 60 (0); the labial cingulum of the lower molars is always absent 159 (3). *Amynodontopsis* is sister group to *Cadurcotherium*, and they share three synapomorphies (Bremer index = 2): the zygomatic process progressively diverges from the maxilla 37 (0); the presence of a sagittal crest on the basilar process 44 (1); the M3 paracone fold is weak 289 (1). *Amynodontopsis jiuyuanensis* has six autapomorphies: nasal notch is above P1-3 (3 (0); nasal bones are long 26 (0); paraoccipital process of the occipital is little developed 48 (1); upper molars antecrochet is usually present 110 (2); M1-2 metastyle is long 120 (1); M1-2 posterior part of the ectoloph is concave 122 (1). *Cadurcotherium* is supported by two synapomorphies (Bremer index = 2): the upper molars lingual cingulum is always absent 114 (3); the lower molars hypolophid is almost sagittal 161 (2). *Cadurcotherium cayluxi* is defined by two autapomorphies: the M1 postfossette is present 127 (0); the m3 talonid is equal or smaller than trigonid 288 (0). *Cadurcotherium minum* is defined by one autapomorphy: upper premolars labial cingulum is always absent 83 (3).

Cadurcodon is placed as a sister group to the clade formed by *Cadurcotherium* and *Amynodontopsis*. *Cadurcodon* is supported by six unambiguous synapomorphies (Bremer index = 2): the ramus coronoid process is little developed 61 (1); the I1 is absent 71 (1); the i1 is absent 76 (1); the upper molars antecrochet is usually absent 110 (1); the upper

postcanine diastema is short 291 (1); the I3 size is distinctly smaller to I2 293 (2).

DISCUSSION

PHYLOGENETIC RELATIONSHIPS

Our results differ strongly from those obtained by the two analyses of Bai *et al.* (2020) in the arrangement of the branches of the different families. Here, and as in Wang *et al.* (2016, 2018) Paraceratheriidae are sister group of the Amynodontidae, whereas in both analyses (parsimony and Bayesian) of Bai *et al.* (2020), they are sister group of the Rhinocerotidae. Besides, in our analysis, Rhinocerotidae (+ *Hyrachys*) are part of a basal trichotomy, which differs from the results of Wang *et al.* (2016, 2018). Furthermore, according to Bai *et al.* (2020), *Hyrachys* could be considered as the earliest-branching representative of Rhinocerotoidea *sensu stricto*, whereas in our results it is placed as sister-group to the Rhinocerotidae.

These differences could obviously be explained by the widely different taxonomic sampling of the analyses, which is centered on Amynodontidae in our case, but on early Ceratomorpha Wood, 1937 for Bai *et al.* (2020), as well as by the nature of the two matrices. Indeed, the morphological matrix from Bai *et al.* (2020) only includes cranial and dental characters (which are more commonly preserved in early Ceratomorpha), whereas ours includes numerous postcranial characters as well, thus possibly leading to the expression of a different evolutionary signal. For example, the clade formed by *Hyrachys* and Rhinocerotidae is supported by seven unambiguous synapomorphies, three of which are postcranial characters. Likewise, the Paraceratheriidae are united with the Amynodontidae based on seven unambiguous synapomorphies, which also include three postcranial characters. Thus, we believe that future analyses that will combine both a large-scale taxonomic sampling, as in Bai *et al.* (2020), and the inclusion of postcranial characters might resolve some of the inconsistencies observed in these different results, which was also suggested by these authors.

The group, composed of Eggysodontidae, *Hyracodon nebraskensis*, Paraceratheriidae which formerly formed the family "Hyracodontidae" (now considered as paraphyletic; Wang *et al.* 2016; Tissier *et al.* 2018), remains paraphyletic in our study (Fig. 7). Some differences can be observed with the tree obtained by the previous analysis of Tissier *et al.* 2018: *Teletaceras radinskyi* is here less derived and closer to the Rhinocerotidae (in fact it should belong to this family, based on the phylogeny of Tissier *et al.* 2020, however, the rhinocerotid sampling is too small to branch it within this group) whereas *Hyracodon nebraskensis* is now no more a sister group of the Paraceratheriidae, but slightly more basal (Fig. 7). This may be caused by the different taxonomic sampling.

"*Pappaceras*" *meiomenus*, had been referred to the family Paraceratheriidae by Wang *et al.* (2016). Our result shows that "*P.*" *meiomenus* and Paraceratheriidae do not form a monophyletic group (Fig. 7) and that "*P.*" *meiomenus* is closer to the Amynodontidae, as already proposed by Tissier *et al.* (2018).

The topology of Amynodontidae is congruent with that of Tissier *et al.* (2018), even though our taxonomic sampling is slightly different. Two main clades, Metamynodontini and Cadurcodontini, were recovered (Fig. 7). Metamynodontini are described by Averianov *et al.* (2016) as “the taxon that includes *Metamynodon planifrons* and all the amynodonts that are closer to it than to *Cadurcodon ardynensis*”. In reverse, they define Cadurcodontini as “the taxon that includes *Cadurcodon ardynensis* and all amynodonts that are closer to it than to *Metamynodon planifrons*”. Thus, considering the cladistic results and contrary to what Wall (1980, 1989) had suggested, *Zaisanamynodon* – originally placed in the tribe of Metamynodontini – should belong to the Cadurcodontini instead (Fig. 7). The cladistic analysis of Averianov *et al.* (2016) had already suggested this but did not retrieve the monophyly of the genus. The phylogenetic position of *Zaisanamynodon* and the monophyly of the genus had already been recovered by Tissier *et al.* (2018). The incorporation in the matrix of ZSN-KKS-28-IPB – referred to *Z. borisovi* – supports even further the position of this genus within the Cadurcodontini (Fig. 7).

Tissier *et al.* (2018) showed that *Amynodontopsis* belongs to the Cadurcodontini while Averianov *et al.* (2016) had suggested a more basal position for it. The incorporation into the analysis of the recently described *Amynodontopsis jiyuanensis* supports a position of the genus within the Cadurcodontini (Fig. 7). However, Wang *et al.* (2020) had also suggested that *Amynodontopsis* aff. *bodei* Tissier, Becker, Codrea, Costeur, Fărcaş, Solomon, Venczel & Maridet, 2018 from Romania and Hungary might not belong to this genus, but we did not include it in our taxonomical sampling, due to its incompleteness. As suggested by Wang *et al.* (2020), the specimens referred to it need to be reexamined, considering the discovery of this new species from China.

The incorporation of UNISTRA.2015.0.1106 into the matrix also resolves the generic/specific relationships within the Metamynodontini (Fig. 7). Averianov *et al.* (2016) had not resolved the generic/specific relationships within the Metamynodontini while Tissier *et al.* (2018) suggested that *Paramynodon birmanicus* (Pilgrim & Cotter, 2016) and *Megalamynodon regalis* Scott, 1945 were early-diverging genera of Metamynodontini and that *Sellamynodon zimborensis* (Codrea & Suraru, 1989) and *Metamynodon planifrons* formed a derived clade. Here, we found that (*Paramynodon birmanicus*, *Megalamynodon regalis*) and (*Sellamynodon zimborensis*, *Metamynodon planifrons*) form two sister clades.

CRANIAL ANATOMY OF THE CADURCODONTINI AND METAMYNODONTINI

Wall (1980) has already shown evidence for a proboscis in Amynodontidae. This structure appeared in Cadurcodontini and would have had the function of locating and manipulating food, reminding the proboscis of tapirs (Wall 1980). *Cadurcodon* presents the greatest number of cranial specializations likely to be associated with the presence of a proboscis (Wall 1980). Following this hypothesis, *Amynodontopsis* also had a well-developed proboscis but less extreme than *Cadurcodon* (Wall 1980). *Cadurcotherium* and *Zaisanamynodon* share with

the Cadurcodontini cranial characters suggesting the position, the movement, and the musculature required for the presence of a proboscis, notably, “the well-developed preorbital fossa” or “the reduction in length of the nasal and of the preorbital region” (Belyaeva 1971; Wall 1980; de Bonis 1995; Lucas *et al.* 1996; Lucas 2006; Ménouret 2018; Tissier *et al.* 2018). These characters are not as derived as in *Amynodontopsis-Cadurcodon*, but *Cadurcotherium-Zaisanamynodon* are much more similar in their skull morphology to Cadurcodontini than to Metamynodontini. The specialization of the facial region to the presence of a proboscis seems to appear gradually in Cadurcodontini, with *Cadurcodon* having the most derived characters. Wall (1980) indicates that *Tapirus* Brisson, 1762 and *Cadurcodon* have cranial similarities, associated with the presence of a proboscis. *Tapirus terrestris*, like the Cadurcodontini, has “the nasal bone length reduced and the nasal incision back of the P4-M1” (Antoine *et al.* 2010). For *Tapirus*, Antoine (2002) relates the elongation (backwards) of the nasal incision to the adaptation of the peri-nasal region to the presence of a proboscis. This also supports the similarities in structure and function of the proboscis between tapirs and Cadurcodontini.

Metamynodontini also show some characters that may suggest the presence of a proboscis: “reduction of the length of the nasal” in *Paramynodon* and *Metamynodon* (Scott & Osborn 1887; Colbert 1938; Scott 1941; see UNISTRA.2015.0.1106), the “maxilla-frontal contact” is present in *Metamynodon* (Scott & Osborn 1887) and “the length of the preorbital region” is reduced in *Metamynodon*, while it is longer in *Paramynodon* (Scott & Osborn 1887; Colbert 1938; Wall 1980). However, “the limit of the nasal incision” is in front of the upper premolars and the preorbital fossa is much less developed in *Paramynodon* and *Metamynodon* than in Cadurcodontini (Colbert 1938; Wall 1980; see UNISTRA.2015.0.1106). These characters, therefore, do not constitute a specialization of the facial region to the presence of a proboscis but rather the existence of a sort of prehensile upper lip in Metamynodontini (Wall 1980). This enlarged mobile lip would have been adapted to seize food, reminding the prehensile upper lip of the African black rhinoceros or the giraffe (Wall 1980).

This specialization of the skull into a proboscis would explain the divergence between the two tribes (Wall 1980). On the one hand, the conservation of an ancestral form of the skull of Amynodontidae by Metamynodontini (as in *Sharamynodon* Kretzoi, 1942). They would have been endowed of a prehensile upper lip rather than a proboscis. On the other hand, Cadurcodontini could have developed a specialization of the skull, the proboscis, related to foraging as in tapirs (Wall 1980).

GEOGRAPHICAL DISTRIBUTION OF AMYNODONTIDAE

Amynodontidae are a family spanning the middle Eocene-Oligocene interval (Fig. 8; Appendix 6). They were highly diversified in the middle Eocene in Asia and North America, as well as in Eastern Europe, but did not appear in Western Europe until the early Oligocene (Wall 1989; Tissier *et al.* 2018).

The Metamynodontini and Cadurcodontini both have an Holarctic distribution, but *Amynodontopsis* and *Zai-*

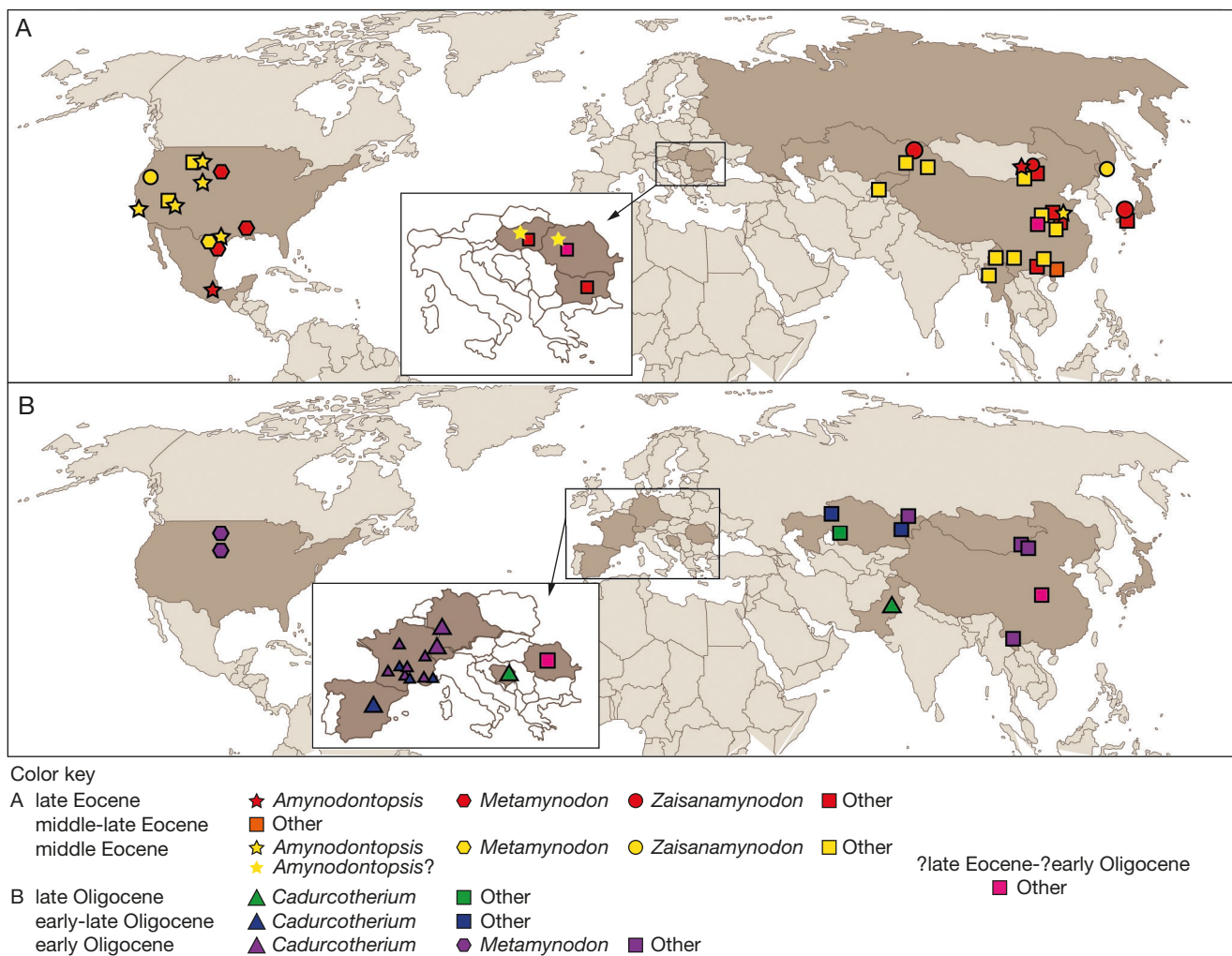


FIG. 8. — Temporal and geographical distribution maps of Amynodontidae Scott & Osborn, 1883 in Eurasia and North America: **A**, middle to late Eocene; **B**, Oligocene. See Appendix 6 for references of the occurrences.

sanamynodon are the only two genera of Amynodontidae that are present both in Asia and North America. Tissier *et al.* (2018) had also reported an earliest occurrence of *Amynodontopsis* in Eastern Europe, with a suspected middle Eocene age, but its identification remains debated (Wang *et al.* 2020). However, the recent description of *Amynodontopsis jiyuanensis* documents a new early occurrence of the genus on the Asian landmass during the middle Eocene and shows that *Amynodontopsis* seems to have first emerged in Asia and later immigrated to North America (Wang *et al.* 2020). Conversely, *Zaisanamynodon* is present since the middle Eocene both in North America and Asia (Fig. 8).

Metamynodon is restricted to the North American landmass, from the middle Eocene to the early Oligocene (Fig. 8) whereas its sister-genus, *Sellamynodon*, is only documented in Eastern Europe, from a single locality (Tissier *et al.* 2018).

Cadurcotherium is mainly documented in Europe (mainly France) during the Oligocene (Fig. 8). Its presence in Western Europe after the Eocene-Oligocene transition would have been related to the “Grande Coupure” event described by Stehlin (1909). This biogeographic event is marked by a large

extinction of endemic Eocene mammals and the immigration of new taxa from Asia (Stehlin 1909) as the consequence of a climatic change related to the Oi-1 glaciation at the beginning of the Oligocene, involving a drop of the sea level (Legendre 1989; Zachos *et al.* 2001; Hooker *et al.* 2004). *Cadurcotherium* is recorded in South Asia throughout the Oligocene epoch, with *Cadurcotherium indicum*; Antoine *et al.* 2004; Métais *et al.* 2009).

CONCLUSION

The inclusion in the matrix of the new material ZSN-KKS-28-IPB (*Zaisanamynodon borisovi*), UNISTRA.2015.0.1106 (*Metamynodon planifrons*) and *Amynodontopsis jiyuanensis*, but also the revised coding of two species assigned to *Cadurcotherium* provide a more exhaustive sampling compared to the previous phylogenetic analyses of Amynodontidae. The obtained cladogram gives a new and more solid phylogenetic hypothesis, especially in distinguishing two main tribes Cadurcodontini and Metamynodontini. However, a revision

of “*Pappaceras*” *meiomenus* would be necessary to determine its position as basal or sister taxon of Amynodontidae. The future study of postcranial material of Amynodontidae, which remains greatly understudied, could improve our understanding of the relationships between Amynodontidae taxa as well as further their relationship within Rhinocerotoidea. The ecology of the family is also very poorly known. Analyses on long bones could permit to understand morphological and anatomical bone adaptations to an aquatic lifestyle, notably for several species suspected of semi-aquatic habits.

Acknowledgements

We sincerely thank Kévin Janneau (“Jardin des sciences de l’Université de Strasbourg”/“Collections de l’École et Observatoire des Sciences de la Terre de Strasbourg, Université de Strasbourg”, France), Olivier Maridet (JURASSICA Museum, Switzerland), Prof. David Lordkipanidze and Prof. Vyacheslav Chkhikvadze† (Georgian National Museum, Georgia) for having provided access to the collections. We are grateful to Olivier Maridet and Jérémie Anquetin (JURASSICA Museum, Switzerland) for valuable help and discussion. We also thank Pierre-Olivier Antoine and two other anonymous reviewers, as well as the editors and staff, at *Comptes Rendus Palevol*, Michel Laurin, Adenise Lopes, Audrina Neveu, Lorenzo Rook, for their very helpful comments on the early version of the manuscript. This project was financially supported by the Swiss National Science Foundation (SNF projects 200021_162359 and P2FRP2_199605).

REFERENCES

- ANTOINE P.-O. 2002. — *Phylogénie et évolution des Elasmotheriina (Mammalia, Rhinocerotoidea)*. Muséum national d’Histoire naturelle (coll. Mémoires du Muséum national d’Histoire naturelle; 188), Paris, 369 p.
- ANTOINE P.-O., SHAH S. M. I., CHEEMA I. U., CROCHET J.-Y., DE FRANCESCHI D., MARIVAUX L., MÉTAIS G. & WELCOMME J.-L. 2004. — New remains of the baluchithere *Paraceratherium bugtiense* (Pilgrim, 1910) from the Late/latest Oligocene of the Bugti Hills, Balochistan, Pakistan. *Journal of Asian Earth Sciences* 24 (1): 71-77. <https://doi.org/10.1016/j.jaes.2003.09.005>
- ANTOINE P.-O., DOWNING K. F., CROCHET J.-Y., DURANTHON F., FLYING L. J., MARIVAUX L., MÉTAIS G., RAHIM-RAJPAR A. & ROOHI G. 2010. — A revision of *Aceratherium blanfordi* Lydekker, 1884 (Mammalia: Rhinocerotoidea) from the Early Miocene of Pakistan: postcranials as a key. *Zoological Journal of the Linnean Society* 160 (1): 139-194. <https://doi.org/10.1111/j.1096-3642.2009.00597.x>
- AVERIANOV A. O. & GODINOT M. 2005. — Ceratomorphs (Mammalia, Perissodactyla) from the early Eocene Andarak 2 locality in Kyrgyzstan. *Geodiversitas* 27 (2): 221-237.
- AVERIANOV A., DANILOV I., JIN J. & WANG Y. 2016. — A new amynodontid from the Eocene of South China and phylogeny of Amynodontidae (Perissodactyla: Rhinocerotoidea). *Journal of Systematic Palaeontology* 15 (11): 927-945. <https://doi.org/10.1080/14772019.2016.1256914>
- BAI B., MENG J., ZHANG C., GONG Y.-X. & WANG Y.-Q. 2020. — The origin of Rhinocerotoidea and phylogeny of Ceratomorpha (Mammalia, Perissodactyla). *Communications Biology* 3: 509. <https://doi.org/10.1038/s42003-020-01205-8>
- BECKER D. 2009. — Earliest record of rhinocerotoids (Mammalia: Perissodactyla) from Switzerland: systematics and biostratigraphy. *Swiss Journal of Geosciences* 102: 489-504. <https://doi.org/10.1007/s0015-009-1330-4>
- BELYAEVA E. I. 1971. — New data on the amynodonts of the USSR. *Trudy Paleontologicheskogo Instituta, Akademija Nauk SSSR* 130: 39-61 [in Russian].
- BENTON R. C., TERRY JR D. O., EVANOFF E. & McDONALD H. G. 2015. — 2. Sedimentary Geology of the Big Badlands, in FARLOW J. O. (ed.), *The White River Badlands: Geology and Paleontology*. Indiana University Press, Indiana: 14-42.
- BIRYUKOV M. D. 1961. — Marsh rhinoceros (Amynodontidae) from the middle Oligocene of Turgai Depression. *Materialy po Istorii Fauny i Flory Kazakhstana* 3: 20-29 [in Russian].
- BONIS L. DE 1995. — Le Garouillas et les sites contemporains (Oligocène, MP 25) des Phosphorites du Quercy (Lot, Tarn-et-Garonne, France) et leurs faunes de vertébrés. 9. Perissodactyla: Amynodontidae. *Palaeontographica Abteilung A: Palaeozoologie, Stratigraphie* 236 (1-6): 157-175. <https://doi.org/10.1127/pala/236/1995/157>
- BORISOV B. A. 1963. — Stratigraphy of the Upper Cretaceous and Paleogene-Neogene of the Zaysan Basin. *Proceedings of the Pansoviet Geological Research Institution (VSEGEI). New series*. 94: 1-70 [in Russian].
- CHOW M.-C. 1957. — On some Eocene and Oligocene mammals from Kwangsi and Yunnan. *Vertebrata PalAsiatica* 1 (3): 201-218.
- CHOW M.-C. & XU Y.-X. 1965. — Amynodonts from the upper Eocene of Honan and Shansi. *Vertebrata PalAsiatica* 9 (2): 190-203.
- COLBERT E. H. 1938. — Fossil mammals from Burma in the American Museum of Natural History. *Bulletin American Museum of Natural History* 74 (6): 255-436. <http://hdl.handle.net/2246/372>
- CRUSAFONT PAIRÓ M. & AGUIRRE E. 1973. — El Arenoso (Carrascosa del Campo, Cuenca): Primera fauna española de Vertebrados del Estampiente superior. *Boletín de la Real Sociedad Española de Historia Natural* 71: 21-28.
- DASHZEVEG D. 1996. — A New Hyracodontid (Perissodactyla, Rhinocerotoidea) from the Ergilin Dzo Formation (Oligocene, Quarry 1) in Dzamyn Ude, Eastern Gobi Desert, Mongolia. *American Museum Novitates* 3178: 1-12. <http://hdl.handle.net/2246/3634>
- EMRY R. J., LUCAS S. G., TYUTKOVA L. & WANG B. 1998. — The Ergilian-Shandgolian (Eocene-Oligocene) transition in the Zaysan Basin, Kazakhstan. *Bulletin of Carnegie Museum of Natural History* 34: 298-312.
- FORTELIUS M. & KAPPELMAN J. 1993. — The largest land mammal ever imagined. *Zoological Journal of the Linnean Society* 108 (1): 85-101. <https://doi.org/10.1111/j.1096-3642.1993.tb02560.x>
- GILLET S. 1960. — À propos de l’Amynodontidé des collections de l’institut de Géologie de l’Université de Strasbourg. *Bulletin du Service de la carte géologique d’Alsace et de Lorraine* 13 (4): 165-168.
- GILLET S., WERNET P. & KOULMANN J. 1957. — Catalogue des exemplaires de Rhinocerotoidea du musée de l’institut de géologie de Strasbourg. *Bulletin du Service de la carte géologique d’Alsace et de Lorraine* 10 (2): 61-74.
- GOLOBOFF P. A., FARRIS J. S. & NIXON K. C. 2008. — TNT, a free program for phylogenetic analysis. *Cladistics* 24 (5): 774-786. <https://doi.org/10.1111/j.1096-0031.2008.00217.x>
- GROMOVA V. 1954. — Mars rhinoceroses (Amynodontidae) of Mongolia. *Trudy Paleontologicheskogo Instituta, Akademija Nauk SSSR* 55: 85-189 [in Russian].
- GROMOVA V. 1960. — The first discovery of amynodonts in the Soviet Union (new genus *Procadurcodon*). *Trudy Paleontologicheskogo Instituta, Akademija Nauk SSSR* 77: 28-151 [in Russian].
- HEISSIG K. 1969. — Die Rhinocerotidae (Mammalia) aus der ober-oligozänen Spaltenfüllung von Gaimersheim. *Abhandlungen der Bayerischen Akademie der Wissenschaften, Mathematisch-Naturwissenschaftliche Klasse, Neue Folge* 138: 1-133.

- HOOKER J. J., COLLINSON M. E. & SILLE N. P. 2004. — Eocene-Oligocene mammalian faunal turnover in the Hampshire Basin, UK: calibration to the global time scale and the major cooling event. *Journal of the Geological Society of London* 161 (2): 161-172. <https://doi.org/10.1144/0016-764903-091>
- HUANG X. & WANG J. 2001. — New materials of tapiroid and rhinocerotoid remains (Mammalia, Perissodactyla) from the middle Eocene of Yuanqu Basin, central China. *Vertebrata PalAsiatica* 39 (3): 197-203.
- JIMÉNEZ-HIDALGO E., SMITH K. T., GUERRERO-ARENAS R. & ALVARADO-ORTEGA J. 2015. — The first Late Eocene continental faunal assemblage from tropical North America. *Journal of South American Earth Sciences* 57: 39-48. <https://doi.org/10.1016/j.jsames.2014.12.001>
- KRETZOI M. 1940. — Alttertiäre Perissodactylen aus Ungarn. *Annales Musei Nationalis Hungarici* 33: 87-99.
- KRETZOI M. 1942. — Ausländische Säugetierfossilien der ungarischen Museen. *Földtani Közlöny* 72 (1-3): 139-148.
- LEGENDRE S. 1989. — Les communautés de mammifères du Paléogène (Éocène supérieur et Oligocène) d'Europe occidentale : structures, milieux et évolution. *Münchner Geowissenschaftliche Abhandlungen. Reihe A: Geologie und Paläontologie* 16: 1-110.
- LI Q. 2003. — New materials of Sianodon from Shaanxi, China. *Vertebrata PalAsiatica* 41 (3): 203-210.
- LUCAS S. G. 2006. — A new amynodontid (Mammalia, Perissodactyla) from the Eocene Clarno Formation, Oregon, and its biochronological significance. *PaleoBios* 26 (2): 7-20.
- LUCAS S. G. & EMRY R. J. 1996. — Biochronological significance of Amynodontidae (Mammalia, Perissodactyla) from the Paleogene of Kazakhstan. *Journal of Paleontology* 70 (4): 691-696. <https://doi.org/10.1017/S0022336000023647>
- LUCAS S. G. & EMRY R. J. 2001. — *Sharamynodon* (Mammalia: Perissodactyla) from the Eocene of the Ily Basin, Kazakhstan and the antiquity of Asian amynodonts. *Proceedings of the Biological Society of Washington* 114: 517-525.
- LUCAS S. G., EMRY R. J. & BAYSHASHOV B. U. 1996. — *Zaisanamyndon*, a late Eocene amynodontid (Mammalia, Perissodactyla) from Kazakhstan and China. *Tertiary Research* 17: 51-58.
- LUCAS S. G., BRAY E. S., EMRY R. J. & HIRSCH K. F. 2012. — Dinosaur eggshell and the Cretaceous-Paleogene Boundary in the Zaysan Basin, Eastern Kazakhstan. *Journal of Stratigraphy* 36 (2): 417-439.
- MALEZ M. & THENIUS E. 1985. — Über das Vorkommen von Amynodonten (Rhinocerotoidea, Mammalia) im Oligo-Miozän von Bosnien (Jugoslawien). *Paleontologia Jugoslavica* 34: 1-26.
- MÉNOURET B. 2018. — Le genre *Cadurcotherium* (Rhinocerotoidea) en Europe ; synthèse des connaissances et révision systématique. *Revue de Paléobiologie* 37 (2): 495-517.
- MÉNOURET B., CHÂTEAUNEUF J.-J., NURY D. & PEIGNÉ S. 2015. — Aubenas-les-Alpes, a forgotten Oligocene site in Provence (S-E France). Part I - Carnivora, Perissodactyla and Microflora. *Annales de Paléontologie* 101 (3): 241-250. <https://doi.org/10.1016/j.anpal.2015.06.002>
- MÉTAIS G., ANTOINE P.-O., BAQRI S. R. H., MARIVAUX L. & WELCOMME J.-L. 2009. — Lithofacies, depositional environments, regional biostratigraphy, and age of the Chitarwata Formation in the Bugti Hills, Balochistan, Pakistan. *Journal of Asian Earth Sciences* 34 (2): 154-167. <https://doi.org/10.1016/j.jseas.2008.04.006>
- MIYATA K., TOMIDA Y., BEARD K. C., GUNNELL G. F., UGAI H. & HIROSE K. 2011. — Eocene mammals from the Akasaki and Nakakoshiki formations, western Kyushu, Japan: Preliminary work and correlation with Asian Land Mammal Ages. *Vertebrata PalAsiatica* 49 (1): 53-68.
- NIKOLOV I. & HEISSIG K. 1985. — Fossile Saugertiere aus dem Obereozan und Unteroligozan Bulgariens und Bedeutung für die Palaeogeographie. *Mitteilungen der Bayerischen Staatssammlung für Paläontologie und Historische Geologie* 25: 61-79.
- OGG J. 2020. — TS Creator visualization of enhanced Geologic Time Scale 2016 database (Version 7.4) (database coordinator): <https://timescalefoundation.org/tscreator/index/index.php>
- OSBORN H. F. 1936. — *Amyodon mongoliensis* from the Upper Eocene of Mongolia. *American Museum Novitates* 859: 1-9. <http://hdl.handle.net/2246/2158>
- PROTHERO D. R. & EMRY R. J. 2004. — The Chadronian, Orellan, and Whitneyan North America Land Mammal Ages, in WOOD-BURNE M. O. (ed.), *Late Cretaceous and Cenozoic Mammals of North America: Biostratigraphy and Geochronology*. Columbia University Press, New York: 156-168.
- ROMAN F. & JOLEAUD L. 1909. — Le *Cadurcotherium* de l'Isle-sur-Sorgues et révision du genre *Cadurcotherium*. *Archives du Muséum d'histoire naturelle de Lyon* 10: 1-52.
- RUSSELL D. & ZHAI R. 1987. — *The Paleogene of Asia: mammals and stratigraphy*. Muséum national d'Histoire naturelle (coll. Mémoires du Muséum national d'Histoire naturelle, Sér. C – Sciences de la Terre (1950-1992); 52), Paris, 490 p.
- SCOTT W. B. 1941. — The Mammalian Fauna of the White River Oligocene: Part V. Perissodactyla. *Transactions of the American Philosophical Society, New Series* 28 (5): 747-980. <https://doi.org/10.2307/1005518>
- SCOTT W. B. & OSBORN H. F. 1887. — Preliminary account of the fossil mammals from the White River formation contained in the Museum of Comparative Zoology. *Bulletin of the Museum of Comparative Zoölogy at Harvard College* 13 (5): 151-171.
- SORENSEN M. D. & FRANZOSA E. A. 2007. — TreeRot, version 3. Boston University, Boston, MA. Available at: <https://people.bu.edu/msoren/TreeRot.html>
- STEHLIN H. G. 1909. — Remarques sur les faunules de mammifères des couches éocènes et oligocènes du Bassin de Paris. *Bulletin de la Société géologique de France* 9: 488-520.
- SWOFFORD D. L. 2002. — PAUP*. Phylogenetic Analysis Using Parsimony (*and Other Methods). Version 4. Sinauer Associates, Sunderland, Massachusetts.
- TISSIER J., BECKER D., CODREA V., COSTEUR L., FÄRCAŞ C., SOLOMON A., VENCZEL M. & MARIDET O. 2018. — New data on Amynodontidae (Mammalia, Perissodactyla) from Eastern Europe: Phylogenetic and palaeobiogeographic implications around the Eocene-Oligocene transition. *PLoS ONE* 13 (4): 1-35. <https://doi.org/10.1371/journal.pone.0193774>
- TISSIER J., ANTOINE P.-O. & BECKER D. 2020. — New material of *Epiceratherium* and a new species of *Mesaceratherium* clear up the phylogeny of early Rhinocerotidae (Perissodactyla). *Royal Society Open Science* 7 (7): 1-21. <https://doi.org/10.1098/rsos.200633>
- TOMIDA Y. & YAMASAKI T. 1996. — A Large Amynodontid from Karatsu Coal-field, Kyushu, Japan and the Eocene-Oligocene Boundary. *Bulletin du Muséum national d'Histoire naturelle, Section C Sciences de la terre, paléontologie, géologie* 22: 117-131.
- TROXELL E. L. 1921. — New Amyodonts in the Marsh Collection. *American Journal of Science* 2 (7): 21-34. <https://doi.org/10.2475/ajs.s5-2.7.21>
- UHLIG U. 1999. — Die Rhinocerotoidea (Mammalia) aus der unteroligozänen Spaltenfüllung Möhren 13 bei Treuchtlingen in Bayern. *Abhandlungen der Bayerischen Akademie der Wissenschaften, Mathematisch-Naturwissenschaftliche Klasse, Neue Folge* 170: 1-254.
- VANDEBERGHE N., HILGEN F. J., SPEIJER R. P., OGG J. G., GRADSTEIN F. M., HAMMER O., HOLLIS C. J. & HOOKER J. J. 2012. — The Paleogene Period, in GRADSTEIN F. M., OGG J. G. & SCHMITZ M. (eds.), *The Geologic Time Scale 2012*. Vol. 2. Elsevier, Oxford: 855-921.
- VEINE-TONIZZO L., TISSIER J., BUKHSIANIDZE M., VASILYAN D. & BECKER D. 2023. — 3D model related to the publication: Cranial morphology and phylogenetic relationships of Amynodontidae Scott & Osborn, 1883 (Perissodactyla, Rhinocerotoidea). *MorphoMuseum* 7: e139. <https://doi.org/10.18563/journal.m3.139>

- WALL W. P. 1980. — Cranial evidence for a proboscis in *Cadurcodon* and a review of snout structure in the family Amynodontidae (Perissodactyla, Rhinocerotoidea). *Journal of Paleontology* 54 (5): 968-977.
- WALL W. P. 1982a. — Evolution and biogeography of the Amynodontidae (Perissodactyla, Rhinocerotoidea), in MAMET B. & COPELAND M. J. (eds), *Proceedings of the Third North American Paleontological Convention*. McGill University, Toronto: 563-567.
- WALL W. P. 1982b. — The genus *Amynodon* and its relationship to other members of the Amynodontidae (Perissodactyla, Rhinocerotoidea). *Journal of Paleontology* 56 (2): 434-443.
- WALL W. P. 1989. — The phylogenetic history and adaptative radiation of the Amynodontidae, in PROTHERO D. R. & SCHOCH R. M. (eds), *The Evolution of Perissodactyls*. Clarendon Press, Oxford University Press, New York: 341-398.
- WALL W. P. 1998. — Amynodontidae, in JANIS C. M., SCOTT K. M. & JACOBS L. L. (eds), *Evolution of Tertiary mammals of North America*. Vol. 1. *Terrestrial carnivores, ungulates, and ungulatelike mammals*. Cambridge University Press, New York: 583-588.
- WALL W. P. & HEINBAUGH K. L. 1999. — Locomotor adaptations in *Metamynodon planifrons* compared to other amynodontids (Perissodactyla, Rhinocerotoidea). *National Parks Paleontological Research* 4: 8-17.
- WALL W. P. & MANNING E. M. 1986. — *Rostriamynodon grangeri* n. gen., n. sp. of amynodontid (Perissodactyla, Rhinocerotoidea) with comments on the phylogenetic history of Eocene Amynodontidae. *Journal of Paleontology* 60 (4): 911-919. <https://www.jstor.org/stable/1305081>
- WANG B. 1992. — The Chinese Oligocene: a preliminary review of mammalian localities and local faunas, in PROTHERO D. R. & BERGGREN W. A. (eds), *Eocene-Oligocene Climatic and Biotic Evolution*. Princeton University Press, Princeton, NJ: 529-547.
- WANG H.-B., BAI B., MENG J. & WANG Y.-Q. 2016. — Earliest known unequivocal rhinocerotoid sheds new light on the origin of Giant Rhinos and phylogeny of early rhinocerotoids. *Scientific reports* 6: 1-9. <https://doi.org/10.1038/s41598-016-0001-8>
- WANG H.-B., BAI B., MENG J. & WANG Y.-Q. 2018. — A New Species of *Forstercooperia* (Perissodactyla: Paraceratheriidae) from Northern China with a Systematic Revision of Forstercooperines. *American Museum Novitates* 3897: 1-41. <https://doi.org/10.1206/3897.1>
- WANG X.-Y., WANG Y.-Q., ZHANG R., ZHANG Z.-H., LUI X.-L. & REN L.-P. 2020. — A new species of *Amynodontopsis* (Perissodactyla: Amynodontidae) from the Middle Eocene of Jiyuan, Henan, China. *Vertebrata PalAsiatica* 58 (3): 1-16. <https://doi.org/10.19615/j.cnki.1000-3118.200313>
- WILSON J. A. & SCHIEBOUT J. A. 1981. — Early tertiary vertebrate faunas Trans-Pecos Texas: Amynodontidae. *The Pearce-Sellards Series* 33: 1-62. <http://hdl.handle.net/2152/29900>
- WOOD H. E. 1937. — A new, lower Oligocene, amynodont rhinoceros. *Journal of Mammalogy* 18 (1): 93-94.
- WOOD H. E. 1941. — Trends in rhinoceros evolution. *Transactions of the New York Academy of Sciences, Series 2* 3 (4): 83-96. <https://doi.org/10.1111/j.2164-0947.1941.tb00783.x>
- XU Y.-X. 1965. — A new genus of amynodont from the Eocene of Lantian, Shensi. *Vertebrata PalAsiatica* 9 (1): 83-86.
- XU Y.-X. 1966. — Amynodonts of Inner Mongolia. *Vertebrata PalAsiatica* 10 (2): 123-190.
- YOUNG C. C. 1937. — An Early Tertiary Vertebrate Fauna from Yuanchü. *Bulletin of the Geological Society of China* 17 (3-4): 413-438. <https://doi.org/10.1111/j.1755-6724.1937.mp173-4012.x>
- ZACHOS J., PAGANI M., SLOAN L., THOMAS E. & BILLUPS K. 2001. — Trends, Rhythms, and Aberrations in Global Climate 65 Ma to Present. *Science* 292 (5517): 686-693. <https://doi.org/10.1126/science.1059412>

Submitted on 2 February 2021;
accepted on 27 January 2022;
published on 20 March 2023.

APPENDICES

APPENDIX 1. — The following appendix is the matrix used to compute the phylogenetic analysis. The matrix consists of 32 terminals scored across 298 anatomical characters. A version of the data matrix executable in Mesquite/PAUP* (.nexus) and the same version executable in TNT (.tnt): https://doi.org/10.5852/cr-palevol2023v22a8_s1

APPENDIX 2. — The following appendix is the detailed list of the 298 characters used to score the 32 terminals considered in the cladistic analysis. The characters 1–282 are from the sequence of Antoine (2002), including the characters 36, 60, 103 and 140 modified from the original sequence to form morphoclines by Tissier *et al.* (2018). The characters 283–289 are from Tissier *et al.* (2018). The characters 290–297 are based on the characters 8, 9, 16, 23, 25, 39, 41 and 45 of Averianov *et al.* (2016). The character 298 is newly included here.

- 1** Nasal: lateral apophysis = 0, absent; 1, present
2 Maxillary: foramen infraorbitalis = 0 above premolars; 1, above molars
3 Nasal incision = 0, above P1-3; 1, above P4-M1
4 Nasal septum = 0, never ossified; 1, ossified (even sometimes)
5 Nasal septum: ossified = 0, partial; 1, complete
6 Nasal/lacrymal: contact = 0, long; 1, punctual or absent
7 Orbit: anterior border = 0, above P4-M2; 1, above M3; 2, behind M3
8 Lacrymal: lacrymal process = 0, present; 1, absent
9 Frontal: processus postorbitalis = 0, present; 1, absent
10 Maxilla: anterior base of the zygomatic process = 0, high; 1, low
11 Zygomatic arch = 0, low; 1, high; 2, very high
12 Zygomatic arch: processus postorbitalis = 0, present; 1, absent
13 Zygomatic arch: processus postorbitalis = 0, on jugal; 1, on squamosal
14 Jugal/squamosal: suture = 0, smooth; 1, rough
15 Skull: dorsal profile = 0, flat; 1, concave; 2, very concave
16 Sphenoid: foramen sphenorbitale and f. rotundum = 0, distinct; 1, fused
17 Squamosal: area between temporal and nuchal crests = 0, flat; 1, depression
18 External auditory pseudomeatus = 0, open; 1, partially closed; 2, closed
19 Occipital side = 0, inclined forward; 1, vertical; 2, inclined backward
20 Occipital: nuchal tubercle = 0, little developed; 1, developed; 2, very developed
21 Skull: back of teeth row = 0, in the posterior half; 1, restricted to the anterior half
22 Pterygoid: posterior margin = 0 nearly horizontal; 1, nearly vertical
23 Skull = 0, dolichocephalic ($I/L \times 100 < 50$); 1, brachycephalic ($I/L \times 100 > 50$)
24 Nasal bones: rostral end = 0, narrow; 1, broad; 2, very broad
25 Nasal bones = 0, totally separated; 1, anteriorly separated; 2, fused
26 Nasal bones = 0, long; 1, short; 2, very long
27 Median nasal horn = 0, absent; 1, present
28 Median nasal horn = 0, small; 1, developed
29 Paired nasal horns = 0, absent; 1, present
30 Paired nasal horns = 0, terminal bumps; 1, lateral crests
31 Frontal horn = 0, absent; 1, present
32 Frontal horn = 0, small; 1, huge
33 Orbit: lateral projection = 0, absent; 1, present
34 Zygomatic width/frontal width = 0, less than 1.5; 1, more than 1.5
35 Frontal-parietal = 0, sagittal crest; 1, close frontoparietal crests; 2, distant crests
36 Occipital crest = 0, straight; 1, concave; 2, forked
37 Maxillary: processus zygomaticus maxillari, anterior tip = 0, progressive; 1, brutal
38 Vomer = 0, acute; 1, rounded
39 Squamosal: articular tubercle = 0, smooth; 1 high
40 Squamosal: transversal profile of articular tubercle = 0, straight; 1, concave
41 Squamosal: foramen postglenoideum = 0, distant from the processus postglenoidalis; 1, close to it
42 Squamosal: processus postglenoidalis = 0, flat; 1, convex; 2, dihedron
43 Basioccipital: foramen nervi hypoglossi = 0, in the middle of the fossa; 1 shift anteroexternally
44 Basioccipital: sagittal crest on the basilar process = 0, absent; 1, present
45 Squamosal: posterior groove on the processus zygomaticus = 0, absent; 1, present
46 Squamosal-occipital: processus post-tympanicus and processus paraoccipitalis = 0, fused; 1, distant
47 Squamosal: processus post-tympanicus = 0, well developed; 1, little developed; 2, huge
48 Occipital: processus paraoccipitalis = 0, well developed; 1, little developed
49 Occipital: foramen magnum = 0, circular; 1, subtriangular
50 Basioccipital: median ridge on the condyle = 0, absent; 1, present
51 Basioccipital: medial truncation on the condyle = 0, absent; 1, present
52 Basioccipital: medial truncation on the condyle = 0, present at juvenile stage; 1, still present at adult stage
53 Symphysis = 0, very upraised; 1, upraised; 2, nearly horizontal
54 Symphysis = 0, spindly; 1, massive; 2, very massive
55 Symphysis: posterior margin = 0, in front of p2; 1, level of p2-4
56 Foramen mentale = 0, in front of p2; 1, level of p2-4
57 Corpus mandibulae: lingual groove = 0, present; 1, absent
58 Corpus mandibulae: lingual groove = 0, present even in adults; 1, only present in juveniles
59 Corpus mandibulae: base = 0, straight; 1, convex; 2, very convex
60 Ramus = 0, inclined backward; 1, vertical; 2, inclined forward
61 Ramus: processus coronoideus = 0, well developed; 1, little developed
62 Foramen mandibulare = 0, below the teeth neck; 1, above the teeth neck
63 Compared length of the premolars/molars rows = 0, $I\text{P}/M > 50$; 1, $42 < I\text{P}/M \leq 50$; 2, $I\text{P}/M \leq 42$
64 Cheek teeth: enamel foldings = 0, absent; 1, weak; 2, developed; 3, intense
65 Cheek teeth: cement = 0, absent; 1, present
66 Cheek teeth: cement = 0, weak or variable; 1, abundant
67 Cheek teeth: shape of enamel = 0, wrinkled; 1, wrinkled and corrugated; 2, corrugated and arborescent
68 Cheek teeth: crown = 0, low; 1, high
69 Cheek teeth: crown = 0, high; 1, partial hypodonty; 2, subhypodonty; 3, hypodonty

APPENDIX 2. — Continuation.

- 70** Cheek teeth: roots = 0, distinct; 1, joined; 2, fused
- 71** I1 = 0, present; 1, absent
- 72** I1: shape of the crown (cross-section) = 0, almond; 1, oval; 2, halfmoon
- 73** I2 = 0, present; 1, absent
- 74** I3 = 0, present; 1, absent
- 75** C1 = 0, present; 1, absent
- 76** i1 = 0, present; 1, absent
- 77** i1: crown = 0, developed, with a pronounced neck; 1, reduced
- 78** i2 = 0, present; 1, absent
- 79** i2: shape = 0, incisor-like; 1, tusk-like
- 80** i2: orientation = 0, parallel; 1, divergent
- 81** i3 = 0, present; 1, absent
- 82** c1 = 0, present; 1, absent
- 83** Upper premolars: labial cingulum = 0, always present; 1, usually present; 2, usually absent; 3, always absent
- 84** P2-4: crochet = 0, always absent; 1, usually present; 2, always present
- 85** P2-4: crochet = 0, always simple; 1, usually simple; 2, usually multiple
- 86** P2-4: metaloph constriction = 0, absent; 1, present
- 87** P2-4: lingual cingulum = 0, always present; 1, usually present; 2, usually absent; 3, always absent
- 88** P2-4: lingual cingulum = 0, continuous; 1, reduced
- 89** P2-4: postfossette = 0, narrow; 1, wide; 2, posterior wall
- 90** P2-3: antecrochet = 0, always absent; 1, usually absent; 2, usually present; 3, always present
- 91** P1 (in adults) = 0, always present; 1, usually present; 2, always absent
- 92** P1: anterolingual cingulum = 0, present; 1, absent
- 93** P2 = 0, present; 1, absent
- 94** P2: protocone and hypocone = 0, fused; 1, lingual bridge; 2, separated; 3, lingual wall
- 95** P2: metaloph = 0, hypocone posterior to metacone; 1, transverse; hypocone anterior to metacone
- 96** P2: lingual groove = 0, present; 1, absent
- 97** P2: protocone = 0, equal or stronger than the hypocone; 1, less strong than the hypocone
- 98** P2: protoloph = 0, present; 1, absent
- 99** P2: protoloph = 0, joined to the ectoloph; 1, interrupted
- 100** P3-4: medifossette = 0, always absent; 1, usually absent; 2, usually present; 3, always present
- 101** P3-4: constriction of the protocone = 0, always absent; 1, usually absent; 2, usually present; 3, always present
- 102** P3-4: protocone and hypocone = 0, fused; 1, lingual bridge; 2, separated; 3, lingual wall
- 103** P3-4: metaloph = 0, hypocone anterior to metacone; 1, transverse; 2, hypocone posterior to metacone
- 104** P3: protoloph = 0, joined to the ectoloph; 1, interrupted
- 105** P3: crista = 0, always absent; 1, usually absent; 2, usually present; 3, always present
- 106** P3: pseudometaloph = 0, always absent; 1, sometimes present
- 107** P4: antecrochet = 0, always absent; 1, usually absent; 2, usually present; 3, always present
- 108** P4: hypocone and metacone = 0, joined; 1, separated
- 109** Upper molars: labial cingulum = 0, always present; 1, usually present; 2, usually absent; 3, always absent
- 110** Upper molars: antecrochet = 0, always absent; 1, usually absent; 2, usually present; 3, always present
- 111** Upper molars: crochet = 0, always absent; 1, usually absent; 2, usually present; 3, always present
- 112** Upper molars: crista = 0, always absent; 1, usually absent; 2, usually present; 3, always present
- 113** Upper molars: medifossette = 0, always absent; 1, usually absent; 2, usually present
- 114** Upper molars: lingual cingulum = 0, always present; 1, usually present; 2, usually absent; 3, always absent
- 115** M1-2: constriction of the protocone = 0, always absent; 1, usually absent; 2, usually present; 3, always present
- 116** M1-2: constriction of the protocone = 0, weak; 1, strong
- 117** M1-2: paracone fold = 0, present; 1, absent
- 118** M1-2: paracone fold = 0, strong; 1, weak
- 119** M1-2: metacone fold = 0, present; 1, absent
- 120** M1-2: metastyle = 0, short; 1, long
- 121** M1-2: metaloph = 0, long; 1, short
- 122** M1-2: posterior part of the ectoloph = 0, straight; 1, concave
- 123** M1-2: cristella = 0, always absent; 1, usually present; 2, always present
- 124** M1-2: posterior cingulum = 0, continuous; 1, low and reduced
- 125** M1: metaloph = 0, continuous; 1, hypocone isolated
- 126** M1: antecrochet-hypocone = 0, always separated; 1, sometimes joined; 2, always joined
- 127** M1: postfossette = 0, present; 1, usually absent
- 128** M2: protocone, lingual groove = 0, always absent; 1, usually absent; 2, always present
- 129** M2: metaloph = 0, continuous; 1, hypocone isolated
- 130** M2: mesostyle = 0, absent; 1, present
- 131** M2: mesostyle = 0, weak; 1, strong
- 132** M2: antecrochet and hypocone = 0, separated; 1, joined
- 133** M3: ectoloph and metaloph = 0, distinct; 1, fused (ectometaloph)
- 134** M3: shape = 0, quadrangular; 1, triangular
- 135** M3: constriction of the protocone = 0, always absent; 1, usually absent; 2, always present
- 136** M3: protocone = 0, trefoil-shape; 1, indented
- 137** M3: protoloph = 0, transverse; 1, lingually elongated
- 138** M3: posterior groove on the ectometaloph = 0, present; 1, absent
- 139** p2-3: vertical external roughnesses = 0, absent; 1, present
- 140** Lower cheek teeth: ectolophid groove = 0, smooth; 1, developed, U-shaped; 2, angular, V-shaped
- 141** Lower cheek teeth: ectolophid groove = 0, vanishing before the neck; 1, developed until the neck
- 142** Lower cheek teeth: trigonid = 0, angular; 1, rounded
- 143** Lower cheek teeth: trigonid = 0, obtuse or right dihedron; 1, acute dihedron
- 144** Lower cheek teeth: metaconid = 0, joined to the metalophid; 1, constricted
- 145** Lower cheek teeth: entoconid = 0, joined to the hypolophid; 1, constricted
- 146** Lower premolars: lingual opening of the posterior valley = 0, U-shape; 1, narrow, V-shape
- 147** Lower premolars: lingual cingulum = 0, always present; 1, usually present; 2, usually absent; 3, always absent
- 148** Lower premolars: lingual cingulum = 0, reduced; 1, continuous

APPENDIX 2. — Continuation.

- 149** Lower premolars: labial cingulum = 0, present; 1, absent
150 Lower premolars: labial cingulum = 0, continuous; 1, reduced
151 d1/p1 (in adults) = 0, always present; 1, usually present; 2, usually absent; 3, always absent
152 d1: 0, always two-rooted; 1, usually two-rooted; 2, always one-rooted
153 p2 = 0, always present; 1, usually present; 2, always absent
154 p2: paralophid = 0, isolated, spur-like; 1, curved, without constriction
155 p2: paraconid = 0, developed; 1, reduced
156 p2: posterior valley = 0, lingually open; 1, usually closed; 2, always closed
157 Lower molars: lingual cingulum = 0, always present; 1, usually present; 2, usually absent; 3, always absent
158 Lower molars: lingual cingulum = 0, reduced; 1, continuous
159 Lower molars: labial cingulum = 0, always present; 1, usually present; 2, usually absent; 3, always absent
160 Lower molars: labial cingulum = 0, continuous; 1, reduced
161 Lower molars: hypolophid = 0, transverse; 1, oblique; 2, almost sagittal
162 m2–3: lingual groove of the entoconid = 0, absent; 1, present
163 DI1 = 0, present; 1, absent
164 DI2 = 0, present; 1, absent
165 D2: mesostyle = 0, present; 1, absent
166 D3–4: mesostyle = 0, absent; 1, present
167 D2: lingual wall = 0, absent; 1, present
168 D2: secondary folds = 0, absent; 1, present
169 D2: mesoloph = 0, absent; 1, present
170 di1 = 0, present; 1, absent
171 di2 = 0, present; 1, absent
172 Lower milk teeth: constriction of the metaconid = 0, present; 1, absent
173 Lower milk teeth: constriction of the entoconid = 0, absent; 1, present
174 Lower milk teeth: protoconid fold = 0, present; 1, absent
175 d1 (in juveniles) = 0, present; 1, absent
176 d2–3: vertical external roughnesses = 0, absent; 1, present
177 d2–3: ectolophid fold = 0, present; 1, absent
178 d2: anterior groove on the ectolophid = 0, absent; 1, present
179 d2: paralophid = 0, simple; 1, double
180 d2: posterior valley = 0, always open; 1, usually open; 2, usually closed; 3, always closed
181 d3: paralophid = 0, double; 1, simple
182 d3: lingual groove on the entoconid = 0, always absent; 1, usually absent; 2, always present
183 Atlas: outline of the rachidian canal = 0, bulb; 1, mushroom
184 Atlas: alar notch = 0, absent; 1, present
185 Atlas: foramen vertebrale lateralis = 0, absent; 1, present
186 Atlas: condyle-facets = 0, comma-like; 1, kidney-like
187 Atlas: axis-facets = 0, straight; 1, sigmoid; 2, transversally concave (NA)
188 Atlas: foramen transversarium = 0, present; 1, absent
189 Atlas: foramen transversarium = beside the axis-facet; 1, hidden by the axis-facet
190 Scapula = 0, elongated ($1.5 < H/APD \leq 2$); 1, very elongated ($H/APD > 2$); 2, spatula-shaped ($H/APD \leq 1.5$)
191 Scapula: glenoid fossa = 0, oval; 1, medial border straight
192 Humerus: greater trochanter = 0, high; 1, low
193 Humerus: fossa olecrani = 0, high; 1, low
194 Humerus: distal articulation = 0, egg cup (shallow median constriction); 1, diabolo (deep median constriction)
195 Humerus: scar on the trochlea = 0, absent; 1, present
196 Humerus: distal gutter on the epicondyle = 0, absent; 1, present
197 Radius: anterior border of the proximal articulation = 0, straight; 1, M-shaped
198 Radius: medial border of the diaphysis = 0, straight; 1, concave
199 Radius: proximal ulna-facets = 0, always separated; 1, usually separated; 2, usually fused; 3, always fused
200 Radius: insertion of the m. biceps brachii = 0, shallow; 1, deep
201 Radius/ulna = 0, independent; 1, in contact or fused
202 Radius: gutter for the m. extensor carpi = 0, deep and wide; 1, weak
203 Radius/ulna: second distal articulation = 0, absent; 1, present
204 Radius: posterior expansion of the scaphoid-facet = 0, low; 1, high
205 Ulna: angle between diaphysis and olecranon = 0, open; 1, closed
206 Ulna: anterior tubercle on the distal end = 0, absent; 1, present
207 Scaphoid: postero-proximal semilunate-facet = 0, present; 1, absent or contact
208 Scaphoid: trapezium-facet = 0, large; 1, small
209 Scaphoid: magnum-facet in lateral view = 0, concave; 1, straight
210 Scaphoid: comparison between anterior and posterior heights = 0, equal; 1, H ant < H post
211 Semilunate: ulna-facet = 0, absent; 1, present
212 Semilunate: distal border of anterior side = 0, acute; 1, rounded
213 Semilunate: anterior side = 0, keeled; 1, smooth
214 Pyramidal: distal facet for semilunate = 0, symmetric; 1, asymmetric; 2, L-shaped
215 Pyramidal: distal side = 0, triangular; 1, elliptic
216 Trapezoid: proximal border in anterior view = 0, symmetric; 1, asymmetric
217 Magnum: proximal border of the anterior side = 0, nearly straight; 1, concave
218 Magnum: indentation on the medial side = 0, absent; 1, present
219 Magnum: indentation on the medial side = 0, always shallow; 1, usually shallow; 2, always deep
220 Magnum: posterior tuberosity = 0, short; 1, long
221 Magnum: posterior tuberosity = 0, curved; 1, straight
222 Unciform: pyramidal-facet and McV-facet = 0, always separate; 1, usually separate; 2, always in contact
223 Unciform: posterior expansion of the pyramidal-facet = 0, always absent; 1, usually absent; 2, usually present; 3, always present
224 McII: magnum-facet = 0, curved; 1, straight
225 McII: anterior McIII-facet = 0, present; 1, sometimes absent
226 McII: posterior McIII-facet = 0, always absent; 1, usually absent; 2, always present
227 McII: anterior and posterior McIII-facets = 0, separated; 1, fused
228 McII: trapezium-facet = 0, always present; 1, usually present; 2, always absent
229 McII: magnum-facet in anterior view = 0, visible; 1, invisible
230 McIV: proximal facet, outline = 0, trapezoid; 1, pentagonal; 2, triangular
231 McV: 0, functional; 1, vestigial

APPENDIX 2. — Continuation.

- 232** Metacarpals: insertion of the m. extensor carpalis = 0, flat; 1, salient
- 233** Coxal: acetabulum = 0, oval or circular; 1, subtriangular
- 234** Femur: trochanter major = 0, high; 1, low
- 235** Femur: head = 0, hemispheric; 1, medially stiff
- 236** Femur: surface of epiphysis of the head = 0, flat; 1, crescent-shaped
- 237** Femur: fovea capitis = 0, present; 1, absent
- 238** Femur: fovea capitis = 0, high and narrow; 1, low and wide
- 239** Femur: third trochanter = 0, developed; 1, very developed
- 240** Femur: relations between the medial lip of the trochlea and the diaphysis = 0, broken angle; 1, ramp
- 241** Femur: proximal border of the patellar trochlea = 0, curved; 1, straight
- 242** Tibia: anterodistal groove = 0, present; 1, absent
- 243** Tibia: mediolateral gutter (tendon m. tibialis posterior) = 0, always present; 1, usually present; 2, always absent
- 244** Tibia: mediolateral gutter = 0, shallow; 1, deep
- 245** Tibia-fibula = 0, independent; 1, in contact or fused
- 246** Tibia: posterior apophysis = 0, high; 1, low
- 247** Tibia: posterior apophysis = 0, acute; 1, rounded
- 248** Fibula: proximal articulation = 0, low; 1, high
- 249** Fibula: distal end = 0, slender; 1, robust
- 250** Fibula: latero-distal gutter (tendon peronaeus muscles) = 0, shallow; 1, deep
- 251** Fibula: position of the latero-distal gutter = 0, posterior; 1, median
- 252** Astragalus: (transverse diameter/height) ratio = 0, TD/H < 1; 1, 1 < TD/H < 1.2; 2, 1.2 > TD/H
- 253** Astragalus: (anteroposterior diameter/height) ratio = 0, APD/H < 0.65; 1, APD/H ≥ 0.65
- 254** Astragalus: orientation of the fibula-facet = 0, subvertical; 1, oblique
- 255** Astragalus: fibula-facet = 0, flat; 1, concave
- 256** Astragalus: collum tali = 0, high; 1, low
- 257** Astragalus: posterior stop on the cuboid-facet = 0, present; 1, absent
- 258** Astragalus: caudal border of the trochlea, in proximal view = 0, sinuous; 1, nearly straight
- 259** Astragalus: orientation of trochlea/distal articulation = 0, very oblique; 1, same axis
- 260** Astragalus: expansion of the calcaneus-facet 1 = 0, always present; 1, usually present
- 261** Astragalus: expansion of the calcaneus-facet 1 = 0, always wide and low; 1, usually wide and low; 2, always high and narrow
- 262** Astragalus: calcaneus-facet 1 = 0, very concave; 1, nearly flat
- 263** Astragalus: calcaneus-facets 2 and 3 = 0, always independent; 1, usually independent; 2, usually fused; 3, always fused
- 264** Calcaneus: fibula-facet = 0, always absent; 1, usually absent; 2, usually present; 3, always present
- 265** Calcaneus: tibia-facet = 0, always absent; 1, usually absent; 2, always present
- 266** Calcaneus: tuber calcanei = 0, massive; 1, slender
- 267** Calcaneus: insertion of the m. fibularis longus = 0, salient; 1, invisible
- 268** Navicular: cross-section = 0, lozenge; 1, rectangle
- 269** Cuboid: proximal side = 0, oval; 1, triangular
- 270** Ectocuneiform: posterolateral process = 0, weak; 1, developed
- 271** MtIII: proximal border of the anterior side = 0, straight; 1, concave; 2, sigmoid
- 272** MtIII: posterior MtII-facet = 0, present; 1, absent
- 273** MtIII: MtIV-facets = 0, distinct; 1, sometimes joined
- 274** MtIII: distal widening of the diaphysis (in adults) = 0, absent; 1, present
- 275** MtIII: cuboid-facet = 0, absent; 1, present
- 276** MtIII: cuboid-facet = 0, small; 1, large
- 277** MtIV: posteroproximal tuberosity = 0, isolated; 1, pad-shaped and continuous
- 278** Phalanx I for MtIII: symmetric insertions = 0, lateral; 1, nearly anterior
- 279** Limbs = 0, slender; 1, robust (brachypod)
- 280** Metapodials: intermediate relief = 0, high and acute; 1, low and smooth
- 281** Central metapodials: posterodistal tubercle on the diaphysis = 0, absent; 1, present
- 282** Lateral metapodials: insertion of the m. interossei = 0, long; 1, short (does not reach distal half of the shaft)
- 283** C = 0, reduced; 1, developed; 2, strong
- 284** c = 0, reduced; 1, developed; 2, strong
- 285** Preorbital fossa = 0, absent or reduced; 1, present
- 286** Mandible: space between condylar and coronoid processes = 0, short (V-shaped); 1, wide (U-shaped)
- 287** Mandible: condylar process = 0, high; 1, low
- 288** m3 talonid = 0, equal or smaller than trigonid; 1, longer than trigonid
- 289** M3 paracone fold = 0, absent; 1, weak; 2, strong
- 290** Diastema between upper incisors and canine = 0, present; 1, absent
- 291** Upper postcanine diastema = 0, long, similar to length of upper premolars; 1, short
- 292** Orbit, vertical position on skull = 0, approximately at dorsoventral midline; 1, low, due to large size of frontal sinuses; 2, high
- 293** I3, size to I2 = 0, similar; 1, much larger; 2, distinctly smaller
- 294** I3, size to i2 = 0, similar or smaller; 1, much larger
- 295** P3, size and morphology = 0, similar in length with p4 and molariform, with talonid well developed; 1, distinctly shorter than p4 and molariform; 2, distinctly shorter than p4 and premolariform, with talonid reduced or absent
- 296** Upper molars, parastyle = 0, large; 1, reduced
- 297** M3, metastyle direction = 0, posterolingually; 1, posterolabially
- 298** P4 third posterior loph = 0, absent; 1, present

APPENDIX 3. — Body masses were estimated using regression equations for perissodactyls and for ungulates of Legendre (1989) or/and regression equation for Rhinocerotidae Owen, 1845 and for all ungulates of Fortelius & Kappelman (1993).

Taxon	Specimen	a	x (mm ²)	b	Log (Y)	Y (tons)	means x measurements (mm)
Regression equation of perissodactyls of Legendre (1989)							
Zaisanamynodon borisovi	ZSN-KKS-28-IPB Belyaeva, 1971	1.559	2080.5	1.425	6.600	4.0	4.1 surface left m1 (57 × 36.5)
		1.559	2156	1.425	6.624	4.2	— surface right m1 (56 × 38.5)
Regression equation of all ungulates of Legendre (1989)							
Zaisanamynodon borisovi	ZSN-KKS-28-IPB	1.515	2080.5	1.568	6.594	3.9	4.1 surface left m1 (57 × 36.5)
		1.515	2156	1.568	6.624	4.2	— surface right m1 (56 × 38.5)
Regression equations of Rhinocerotidae Gray, 1821 of Fortelius & Kappelman (1993)							
Zaisanamynodon borisovi	ZSN-KKS-28-IPB	3.78	81	-3.33	3.884	7.7	5.7 length left M2
		3.78	81	-3.33	3.884	7.7	— length right M2
		3.5	82.5	-2.98	3.728	5.3	— length right M3
		2.41	284	-2.6	3.312	2.1	— TRLU (upper tooth row length)
Metamynodon planifrons	UNISTRA.2015.0.1106 Scott & Osborn, 1887	3.78	50.5	-3.33	3.108	1.3	1.3 length left M2
		3.78	50	-3.33	3.092	1.2	— length right M2
		3.5	60	-2.98	3.244	1.8	— length left M3
		3.5	60.5	-2.98	3.256	1.8	— length right M3
		3.02	542	-5.21	3.047	1.1	— CBL (basicondylar length)
		2.68	315	-3.6	3.095	1.2	— WZYG (zygomatic width)
		1.6	170730	-5.3	3.072	1.2	— CBL × WZYG
		2.41	199	-2.6	2.940	0.9	— TRLU (upper tooth row length)
	VPM-9157, Holotype measurements from Scott & Osborn (1887)	3.5	60	-2.98	3.244	1.8	1.5 length of M3
		3.02	550	-5.21	3.066	1.2	— CBL (basicondylar length)
		2.68	365	-3.6	3.267	1.8	— WZYG (zygomatic width)
		1.6	200750	-5.3	3.184	1.5	— CBL × WZYG
		2.41	225	-2.6	3.069	1.2	— TRLU (upper tooth row length)
Regression equations of all ungulates of Fortelius & Kappelman (1993)							
Zaisanamynodon borisovi	ZSN-KKS-28-IPB	2.89	81	1.26	6.776	6.0	4.5 length left M2
		2.89	81	1.26	6.776	6.0	— length right M2
		2.66	82.5	1.49	6.588	3.9	— length right M3
		2.99	284	-0.96	6.375	2.4	— TRLU (upper tooth row length)
Metamynodon planifrons	UNISTRA.2015.0.1106	2.89	50.5	1.26	6.183	1.5	1.2 length left M2
		2.89	50	1.26	6.170	1.5	— length right M2
		2.66	60	1.49	6.220	1.7	— length left M3
		2.66	60.5	1.49	6.229	1.7	— length right M3
		3.10	542	-2.69	5.785	0.6	— CBL (basicondylar length)
		3.03	315	-1.52	6.050	1.1	— WZYG (zygomatic width)
		1.57	170730	-2.26	5.955	0.9	— CBL × WZYG
		2.99	199	-0.96	5.914	0.8	— TRLU (upper tooth row length)
	VPM-9157, Holotype measurements from Scott & Osborn (1887)	2.66	60	1.49	6.220	1.7	1.3 length of M3
		3.10	550	-2.69	5.805	0.6	— CBL (basicondylar length)
		3.03	365	-1.52	6.244	1.8	— WZYG (zygomatic width)
		1.57	200750	-2.26	6.065	1.2	— CBL × WZYG
		2.99	225	-0.96	6.073	1.2	— TRLU (upper tooth row length)

APPENDIX 4. — The list of transformations. **Simple arrow** (\rightarrow) indicates an ambiguous change; **double arrow** ($\Rightarrow\Rightarrow$) indicates a synapomorphy/autapomorphy (**green coloured cells**). Data were obtained with the “describe trees” command of PAUP*. See Appendix 5 for corresponding of nodes with the parsimonious tree. Abbreviation: **CI**, consistency index.

Branch	Character	Steps	CI	Change	Branch	Character	Steps	CI	Change
Node 36 --> <i>Tapirus terrestris</i> (Linnaeus, 1758)	3	1	0.200	0 $\Rightarrow\Rightarrow$ 1		278	1	1.000	0 \rightarrow 1
	6	1	0.500	0 $\Rightarrow\Rightarrow$ 1		280	1	1.000	0 $\Rightarrow\Rightarrow$ 1
	10	1	0.167	1 \rightarrow 0		284	1	0.286	1 \rightarrow 0
	11	1	0.250	1 $\Rightarrow\Rightarrow$ 0		286	1	0.200	0 \rightarrow 1
	16	1	0.333	1 \rightarrow 0	Node 37 --> Node 39	47	1	0.667	0 $\Rightarrow\Rightarrow$ 1
	20	1	0.286	1 $\Rightarrow\Rightarrow$ 0		60	1	0.286	1 \rightarrow 2
	22	1	1.000	0 \rightarrow 1		72	1	0.500	0 \rightarrow 1
	26	1	0.333	0 $\Rightarrow\Rightarrow$ 1		95	1	0.250	0 \rightarrow 1
	34	1	0.167	0 $\Rightarrow\Rightarrow$ 1		99	1	0.143	1 \rightarrow 0
	38	1	0.500	1 $\Rightarrow\Rightarrow$ 0		102	1	0.333	0 \rightarrow 1
	40	1	1.000	0 $\Rightarrow\Rightarrow$ 1		108	1	0.250	1 \rightarrow 0
	53	1	0.143	1 \rightarrow 0		109	1	0.200	1 \rightarrow 0
	55	1	0.250	0 $\Rightarrow\Rightarrow$ 1		110	1	0.214	1 $\Rightarrow\Rightarrow$ 2
	56	1	0.167	1 $\Rightarrow\Rightarrow$ 0		118	1	0.143	0 $\Rightarrow\Rightarrow$ 1
	97	1	0.500	0 $\Rightarrow\Rightarrow$ 1		119	1	0.333	0 $\Rightarrow\Rightarrow$ 1
	99	1	0.143	1 \rightarrow 0		144	1	0.333	1 \rightarrow 0
	102	1	0.333	0 \rightarrow 2		147	2	0.429	2 \rightarrow 0
	108	1	0.250	1 \rightarrow 0		283	1	0.400	0 \rightarrow 1
	109	1	0.200	1 \rightarrow 0		287	1	0.333	0 $\Rightarrow\Rightarrow$ 1
	110	1	0.214	1 \rightarrow 0	Node 39 --> Node 40	289	1	0.167	2 $\Rightarrow\Rightarrow$ 1
	142	1	0.333	0 $\Rightarrow\Rightarrow$ 1		37	1	0.143	0 \rightarrow 1
	144	1	0.333	1 \rightarrow 0		55	1	0.250	0 $\Rightarrow\Rightarrow$ 1
	147	2	0.429	2 \rightarrow 0		92	1	1.000	0 \rightarrow 1
	150	1	0.250	0 $\Rightarrow\Rightarrow$ 1		114	1	0.158	2 \rightarrow 3
	151	3	0.300	0 $\Rightarrow\Rightarrow$ 3		121	1	0.167	0 $\Rightarrow\Rightarrow$ 1
	157	2	0.250	2 $\Rightarrow\Rightarrow$ 0		146	1	0.333	1 \rightarrow 0
	160	1	0.250	0 \rightarrow 1		148	1	0.500	0 $\Rightarrow\Rightarrow$ 1
	179	1	0.500	1 \rightarrow 0		151	3	0.300	0 $\Rightarrow\Rightarrow$ 3
	181	1	0.500	0 \rightarrow 1		152	2	0.333	2 \rightarrow 0
	184	1	0.500	1 \rightarrow 0		158	1	0.500	0 \rightarrow 1
	185	1	0.500	0 \rightarrow 1		179	1	0.500	1 \rightarrow 0
	187	1	1.000	0 $\Rightarrow\Rightarrow$ 1		198	1	0.500	0 \rightarrow 1
	209	1	0.500	0 $\Rightarrow\Rightarrow$ 1		201	1	0.333	0 $\Rightarrow\Rightarrow$ 1
	213	1	0.333	1 \rightarrow 0		207	1	0.333	0 $\Rightarrow\Rightarrow$ 1
	238	1	0.333	1 \rightarrow 0		221	1	1.000	0 \rightarrow 1
	244	1	0.500	0 \rightarrow 1		228	2	0.500	0 $\Rightarrow\Rightarrow$ 2
	254	1	0.200	0 $\Rightarrow\Rightarrow$ 1		241	1	0.333	0 \rightarrow 1
	263	1	0.300	1 \rightarrow 0		253	1	0.500	0 \rightarrow 1
	292	1	0.333	0 $\Rightarrow\Rightarrow$ 1		259	1	1.000	0 \rightarrow 1
	293	1	0.400	0 $\Rightarrow\Rightarrow$ 1	Node 40 --> Node 43	263	2	0.300	1 \rightarrow 3
	294	1	0.250	0 \rightarrow 1		24	1	0.333	0 \rightarrow 1
	296	1	0.500	0 $\Rightarrow\Rightarrow$ 1		60	1	0.286	2 \rightarrow 1
Node 36 --> Node 37	42	1	0.400	0 \rightarrow 1		63	1	0.400	0 $\Rightarrow\Rightarrow$ 1
	54	1	0.333	0 $\Rightarrow\Rightarrow$ 1		89	2	0.250	0 $\Rightarrow\Rightarrow$ 2
	70	1	0.500	0 \rightarrow 1		97	1	0.500	0 $\Rightarrow\Rightarrow$ 1
	86	1	0.333	0 $\Rightarrow\Rightarrow$ 1		103	1	0.200	1 \rightarrow 0
	114	2	0.158	0 $\Rightarrow\Rightarrow$ 2		180	3	1.000	0 \rightarrow 3
	120	1	0.125	0 $\Rightarrow\Rightarrow$ 1		183	1	0.500	0 \rightarrow 1
	138	1	0.250	0 \rightarrow 1		185	1	0.500	0 \rightarrow 1
	146	1	0.333	0 \rightarrow 1		190	1	1.000	1 \rightarrow 2
	152	2	0.333	0 \rightarrow 2		191	1	0.500	0 \rightarrow 1
	161	1	0.400	0 $\Rightarrow\Rightarrow$ 1		212	1	0.250	1 $\Rightarrow\Rightarrow$ 0
	173	1	1.000	0 \rightarrow 1		247	1	1.000	0 $\Rightarrow\Rightarrow$ 1
	175	1	1.000	0 \rightarrow 1		252	2	0.500	0 $\Rightarrow\Rightarrow$ 2
	177	1	1.000	0 \rightarrow 1		276	1	1.000	0 \rightarrow 1
	186	1	1.000	0 \rightarrow 1		285	1	1.000	0 $\Rightarrow\Rightarrow$ 1
	190	1	1.000	0 \rightarrow 1	Node 43 --> Node 44	297	1	1.000	0 \rightarrow 1
	192	1	0.500	0 \rightarrow 1		7	1	0.250	0 \rightarrow 1
	197	1	1.000	0 \rightarrow 1		16	1	0.333	1 \rightarrow 0
	208	1	0.500	0 \rightarrow 1		63	1	0.400	1 $\Rightarrow\Rightarrow$ 2
	226	2	0.500	0 \rightarrow 2		67	1	1.000	0 \rightarrow 1
	229	1	0.500	0 \rightarrow 1		88	1	0.500	0 \rightarrow 1
	231	1	0.500	0 $\Rightarrow\Rightarrow$ 1		91	1	0.400	0 $\Rightarrow\Rightarrow$ 1
	258	1	0.500	0 \rightarrow 1		94	1	0.429	2 \rightarrow 0
	261	2	0.333	0 \rightarrow 2		102	1	0.333	1 $\Rightarrow\Rightarrow$ 0
	264	3	1.000	0 $\Rightarrow\Rightarrow$ 3		110	1	0.214	2 $\Rightarrow\Rightarrow$ 1
	265	2	0.667	0 \rightarrow 2		114	2	0.158	3 $\Rightarrow\Rightarrow$ 1
						118	1	0.143	1 $\Rightarrow\Rightarrow$ 0

APPENDIX 4. — Continuation.

Branch	Character	Steps	CI	Change	Branch	Character	Steps	CI	Change
	142	1	0.333	0 --> 1		65	1	0.143	0 --> 1
	143	1	0.500	1 --> 0		288	1	0.333	0 ==> 1
	157	2	0.250	2 --> 0	Node 62 --> Node 61	10	1	0.167	0 ==> 1
	188	1	0.333	0 --> 1		38	1	0.500	1 ==> 0
	199	3	0.333	0 --> 3		53	1	0.143	1 --> 0
	200	1	1.000	0 --> 1		54	1	0.333	1 --> 2
	220	1	0.500	0 --> 1		56	1	0.167	1 --> 0
	231	1	0.500	1 --> 0		60	1	0.286	1 --> 0
	249	1	0.500	0 --> 1		149	1	0.333	0 --> 1
	256	1	0.250	0 --> 1		159	3	0.167	0 --> 3
	270	1	1.000	0 --> 1		289	1	0.167	2 ==> 1
	284	2	0.286	0 --> 2	Node 61 -->	102	1	0.333	0 ==> 2
Node 44 --> Node 45	2	1	0.250	0 --> 1	<i>Metamynodon</i>	111	1	0.500	0 ==> 1
(Amynodontidae	8	1	0.333	0 ==> 1	<i>planifrons</i> Scott &	112	1	0.333	0 ==> 1
Scott & Osborn, 1883)	10	1	0.167	1 ==> 0	Osborn, 1887	120	1	0.125	0 --> 1
	65	1	0.143	0 --> 1	Node 61 --> UNIS-	13	1	1.000	0 ==> 1
	83	2	0.200	0 --> 2	TRA.2015.0.1106	45	1	0.250	0 ==> 1
	86	1	0.333	1 --> 0		99	1	0.143	0 ==> 1
	91	1	0.400	1 ==> 2		103	1	0.200	2 --> 1
	109	3	0.200	1 ==> 2		114	2	0.158	1 ==> 3
	283	1	0.400	1 ==> 2		117	1	1.000	0 ==> 1
	296	1	0.500	0 ==> 1		121	1	0.167	1 ==> 0
Node 45 --> Node 46	7	1	0.250	1 --> 0		292	1	0.333	2 ==> 0
	11	1	0.250	1 ==> 0	Node 60 --> Node 59	37	1	0.143	1 ==> 0
	19	1	0.250	1 ==> 2		61	1	0.333	0 --> 1
	23	1	0.250	0 ==> 1		105	1	0.188	0 --> 1
	34	1	0.167	0 --> 1		212	1	0.250	0 --> 1
	36	1	0.286	1 ==> 0		256	1	0.250	1 --> 0
Node 46 --> Node 47	12	1	0.200	0 --> 1		274	1	0.333	0 --> 1
	20	1	0.286	1 --> 0		290	1	0.200	1 --> 0
	26	1	0.333	0 ==> 1		293	1	0.400	0 ==> 1
	83	1	0.200	2 --> 3	Node 59 -->	48	1	0.250	0 ==> 1
	88	1	0.500	1 --> 0	<i>Megalamyndon</i>	56	1	0.167	1 ==> 0
	89	1	0.250	2 --> 1	<i>regalis</i> Wood, 1945	77	1	0.500	0 ==> 1
	103	1	0.200	0 --> 1		102	1	0.333	0 ==> 2
	155	1	0.333	0 ==> 1		112	1	0.333	0 ==> 1
	165	1	0.500	1 --> 0		284	1	0.286	2 ==> 1
	167	1	1.000	0 --> 1	Node 59 -->	53	1	0.143	1 ==> 0
	289	1	0.167	1 ==> 2	<i>Paramyndon</i>	98	1	0.250	0 ==> 1
	292	1	0.333	0 --> 1	<i>birmanicus</i>	114	1	0.158	1 ==> 0
Node 47 --> Node 58	8	1	0.333	1 --> 0	(Pilgrim & Cotter,	150	1	0.250	0 ==> 1
	65	1	0.143	1 --> 0	2016)	159	2	0.167	0 ==> 2
	110	1	0.214	1 ==> 0		291	1	0.250	1 --> 0
	120	1	0.125	1 --> 0		34	1	0.167	1 --> 0
	140	1	0.400	1 ==> 0	Node 58 --> Node	42	1	0.400	1 ==> 2
	153	2	0.667	0 ==> 2	57 (Cadurcodontini	66	1	1.000	0 --> 1
	290	1	0.200	0 --> 1	Wall, 1982)	83	3	0.200	3 ==> 0
	292	1	0.333	1 --> 2		118	1	0.143	0 --> 1
	295	2	0.286	0 ==> 2		193	1	0.500	0 ==> 1
Node 58 --> Node 60	11	1	0.250	0 ==> 1		198	1	0.500	1 --> 0
(Metamynodontini	42	1	0.400	1 ==> 0		202	1	0.500	0 --> 1
Scott & Osborn, 1887)	103	1	0.200	1 --> 2		245	1	0.500	0 --> 1
	158	1	0.500	1 --> 0		287	1	0.333	1 ==> 0
	194	1	0.500	0 ==> 1		288	1	0.333	0 ==> 1
	195	1	1.000	0 --> 1	Node 57 --> Node 54	10	1	0.167	0 --> 1
	275	1	0.333	0 --> 1		12	1	0.200	1 --> 0
	291	1	0.250	0 --> 1		19	1	0.250	2 --> 1
Node 60 --> Node 62	12	1	0.200	1 --> 0		23	1	0.250	1 ==> 0
	18	2	0.500	0 ==> 2		77	1	0.500	0 --> 1
	39	1	1.000	0 --> 1		124	1	0.500	0 ==> 1
	211	1	0.333	0 --> 1		127	1	0.500	0 ==> 1
	254	1	0.200	0 --> 1		192	1	0.500	1 ==> 0
	255	1	0.500	0 --> 1		238	1	0.333	1 --> 0
	279	1	1.000	0 --> 1		246	1	0.500	0 --> 1
Node 62 -->	11	1	0.250	1 ==> 2		255	1	0.500	0 --> 1
<i>Sellamynodon</i>	15	2	0.500	0 ==> 2		292	1	0.333	2 --> 1
<i>zimborensis</i>	20	1	0.286	0 --> 1		294	1	0.250	0 ==> 1
(Codrea & Suraru,	49	1	0.500	0 ==> 1	Node 54 --> Node 50	11	1	0.250	0 --> 1
1989)	57	1	1.000	0 ==> 1		19	1	0.250	1 --> 0
	60	1	0.286	1 ==> 2		21	1	1.000	0 --> 1

APPENDIX 4. — Continuation.

Branch	Character	Steps	CI	Change	Branch	Character	Steps	CI	Change	
	34	1	0.167	0 --> 1		78	1	0.333	0 --> 1	
	61	1	0.333	0 ==> 1		81	1	0.250	0 --> 1	
	71	1	1.000	0 ==> 1		89	1	0.250	1 --> 2	
	76	1	1.000	0 ==> 1		114	2	0.158	1 ==> 3	
	110	1	0.214	0 ==> 1		149	1	0.333	0 --> 1	
	118	1	0.143	1 --> 0		161	1	0.400	1 ==> 2	
	126	2	1.000	0 --> 2		287	1	0.333	0 --> 1	
	274	1	0.333	0 --> 1	Node 52 --> <i>Cadurcotherium cayluxi</i>	103	1	0.200	0 --> 1	
	291	1	0.250	0 ==> 1	Gervais, 1873	127	1	0.500	1 ==> 0	
	293	1	0.400	0 ==> 2	Node 52 --> <i>Cadurcotherium minum</i>	288	1	0.333	1 ==> 0	
Node 50 --> Node 49	3	1	0.200	1 --> 0	Filhol, 1880	83	3	0.200	0 ==> 3	
	53	1	0.143	1 ==> 0	Node 57 --> Node 56	2	1	0.250	1 --> 0	
	59	1	0.500	0 ==> 1		25	2	0.667	0 --> 2	
	78	1	0.333	0 ==> 1		36	1	0.286	0 --> 1	
	161	1	0.400	1 ==> 2		37	1	0.143	1 ==> 0	
Node 49 --> Node 48	68	1	0.500	0 ==> 1		56	1	0.167	1 --> 0	
	73	1	0.500	0 --> 1		99	1	0.143	0 --> 1	
	74	1	0.250	0 --> 1		109	2	0.200	3 --> 1	
	81	1	0.250	0 --> 1		114	1	0.158	1 ==> 2	
	89	1	0.250	1 --> 2		120	1	0.125	0 --> 1	
	90	3	1.000	0 --> 3		254	1	0.200	0 --> 1	
	102	1	0.333	0 --> 3		256	1	0.250	1 --> 0	
	104	1	0.250	0 --> 1		286	1	0.200	1 --> 0	
	107	3	0.750	0 --> 3		293	1	0.400	0 --> 1	
	111	1	0.500	0 --> 1		298	1	1.000	0 ==> 1	
	114	1	0.158	1 --> 2	Node 56 --> Node 55	53	1	0.143	1 --> 2	
Node 48 --> <i>Cadurcodon kazakademi</i> Biryukov, 1961	286	1	0.200	1 ==> 0		91	1	0.400	2 --> 1	
Node 49 --> <i>Cadurcodon maomingensis</i>	65	1	0.143	0 --> 1		98	1	0.250	0 --> 1	
Averianov, Danilov, Jin & Wang, 2016	121	1	0.167	1 ==> 0		114	1	0.158	2 --> 3	
Node 50 --> <i>Cadurcodon bahoensis</i> (Xu, 1965)	141	1	0.250	0 ==> 1		153	1	0.667	2 --> 1	
Node 54 --> Node 53	8	1	0.333	0 --> 1		289	1	0.167	2 ==> 1	
	24	1	0.333	1 ==> 0		295	1	0.286	2 --> 1	
	60	1	0.286	1 ==> 0	Node 55 --> ZSN-KKS-28-IPB	103	1	0.200	1 ==> 2	
	95	1	0.250	1 --> 0		104	1	0.250	0 ==> 1	
	102	1	0.333	0 --> 2		105	3	0.188	0 ==> 3	
	103	1	0.200	1 --> 0		108	1	0.250	0 ==> 1	
	105	3	0.188	0 --> 3		137	1	1.000	0 ==> 1	
	159	3	0.167	0 ==> 3	Node 56 --> <i>Zaisanamynodon protheroi</i> Lucas, 2006	148	1	0.500	1 ==> 0	
Node 53 --> Node 51	271	1	0.333	2 --> 1		Node 47 --> <i>Sharamynodon mongoliensis</i> (Osborn, 1936)	53	1	0.143	1 ==> 2
	37	1	0.143	1 ==> 0		55	1	0.250	1 ==> 0	
	44	1	0.333	0 ==> 1		70	1	0.500	1 --> 0	
	54	1	0.333	1 --> 0		98	1	0.250	0 ==> 1	
	94	1	0.429	0 --> 2		114	1	0.158	1 ==> 0	
	140	1	0.400	0 --> 1		141	1	0.250	0 ==> 1	
	289	1	0.167	2 ==> 1		209	1	0.500	0 ==> 1	
	290	1	0.200	1 --> 0		271	2	0.333	2 ==> 0	
	295	2	0.286	2 --> 0		283	1	0.400	2 ==> 1	
Node 51 --> <i>Amynodontopsis bodei</i> Stock, 1933	36	1	0.286	0 ==> 1		284	1	0.286	2 ==> 1	
	45	1	0.250	0 ==> 1	Node 46 --> <i>Amynodon advenus</i> (Marsh, 1875)	2	1	0.250	1 --> 0	
	109	3	0.200	3 ==> 0		37	1	0.143	1 ==> 0	
Node 51 --> <i>Amynodontopsis jiyanensis</i> Wang X.-Y., Wang Y.-Q., Zhang R., Zhang Z.-H., Liu & Ren, 2020	3	1	0.200	1 ==> 0		48	1	0.250	0 ==> 1	
	26	1	0.333	1 ==> 0		53	1	0.143	1 ==> 0	
	48	1	0.250	0 ==> 1		60	1	0.286	1 ==> 0	
	110	2	0.214	0 ==> 2		99	1	0.143	0 ==> 1	
	120	1	0.125	0 ==> 1		105	1	0.188	0 ==> 1	
	122	1	0.500	0 ==> 1		150	1	0.250	0 ==> 1	
Node 53 --> Node 52	7	1	0.250	0 --> 1		156	2	1.000	0 ==> 2	
	10	1	0.167	1 --> 0		159	2	0.167	0 ==> 2	
	19	1	0.250	1 --> 2		160	1	0.250	0 ==> 1	
	20	1	0.286	0 --> 1	Node 45 --> <i>Rostriamynodon grangeri</i> Wall & Manning, 1986	56	1	0.167	1 ==> 0	
	25	1	0.667	0 --> 1		110	1	0.214	1 ==> 0	
	65	1	0.143	0 --> 1		120	1	0.125	1 ==> 0	
	68	1	0.500	0 --> 1		140	1	0.400	1 ==> 2	
	74	1	0.250	0 --> 1		293	1	0.400	0 ==> 2	

APPENDIX 4. — Continuation.

Branch	Character	Steps	CI	Change	Branch	Character	Steps	CI	Change
Node 44 --> “Pappaceras”	24	1	0.333	1 --> 0		105	3	0.188	0 ==> 3
<i>meiomenus</i> Wang	45	1	0.250	0 ==> 1		112	2	0.333	0 ==> 2
H.-B., Bai, Meng &	114	1	0.158	1 ==> 0		178	1	1.000	0 ==> 1
Wang Y.-Q., 2016	119	1	0.333	1 ==> 0		181	1	0.500	0 --> 1
	121	1	0.167	1 ==> 0		182	2	1.000	0 ==> 2
Node 43 --> Node 42	3	1	0.200	0 --> 1		275	1	0.333	0 ==> 1
(Paraceratheriidae	15	1	0.500	0 --> 1		283	1	0.400	1 --> 0
Osborn, 1923)	19	1	0.250	1 --> 0		286	1	0.200	1 --> 0
	35	1	0.500	0 --> 1		290	1	0.200	0 ==> 1
	37	1	0.143	1 --> 0	Node 39 --> Node 38	7	1	0.250	0 --> 1
	44	1	0.333	0 --> 1	(Eggyodontidae	11	1	0.250	1 --> 0
	53	1	0.143	1 ==> 2	Breuning, 1923)	53	1	0.143	1 --> 0
	73	1	0.500	0 --> 1		94	1	0.429	2 ==> 1
	74	1	0.250	0 --> 1		103	1	0.200	1 ==> 2
	75	1	0.500	0 --> 1		133	1	0.333	0 ==> 1
	99	1	0.143	0 --> 1		157	2	0.250	2 --> 0
	133	1	0.333	0 ==> 1		160	1	0.250	0 --> 1
	141	1	0.250	0 --> 1		202	1	0.500	0 --> 1
	168	1	1.000	0 --> 1		217	1	0.500	0 --> 1
	169	1	1.000	0 --> 1		249	1	0.500	0 --> 1
	187	1	1.000	0 ==> 2		263	1	0.300	1 --> 0
	229	1	0.500	1 --> 0		268	1	0.500	0 ==> 1
	234	1	1.000	0 --> 1		271	1	0.333	2 --> 1
	241	1	0.333	1 --> 0		283	1	0.400	1 --> 2
	246	1	0.500	0 --> 1		284	2	0.286	0 ==> 2
	263	3	0.300	3 --> 0		291	1	0.250	0 --> 1
	274	1	0.333	0 --> 1	Node 38 -->	63	1	0.400	0 ==> 1
	294	1	0.250	0 --> 1	<i>Allacerops turgaica</i>	89	1	0.250	0 ==> 1
Node 42 --> Node 41	54	1	0.333	1 --> 2	(Borissiak, 1915)	105	3	0.188	0 ==> 3
	65	1	0.143	0 --> 1		140	1	0.400	1 ==> 2
	78	1	0.333	0 ==> 1		141	1	0.250	0 ==> 1
	81	1	0.250	0 ==> 1		155	1	0.333	0 ==> 1
	82	1	0.500	0 ==> 1	Node 38 -->	95	1	0.250	1 --> 0
	138	1	0.250	1 --> 0	<i>Eggyodon osborni</i>	114	2	0.158	2 ==> 0
	159	1	0.167	0 --> 1	Schlosser, 1902	138	1	0.250	1 --> 0
Node 41 -->	11	1	0.250	1 ==> 0		154	1	0.333	1 ==> 0
<i>Paraceratherium</i>	47	1	0.667	1 ==> 2		211	1	0.333	0 ==> 1
<i>bugtiense</i> Forster	48	1	0.250	0 ==> 1		212	1	0.250	1 ==> 0
Cooper, 1911	91	2	0.400	0 ==> 2		224	1	0.500	0 ==> 1
	94	1	0.429	2 ==> 1		256	1	0.250	0 ==> 1
	103	1	0.200	0 --> 1		272	1	0.500	0 ==> 1
	110	1	0.214	2 ==> 3	Node 37 -->	1	1	0.500	0 ==> 1
	124	1	0.500	0 ==> 1	<i>Teletaceras radin-</i>	36	1	0.286	1 ==> 0
	128	2	1.000	0 ==> 2	<i>skyi</i> Hanson, 1989	46	1	0.500	0 ==> 1
	155	1	0.333	0 ==> 1		65	1	0.143	0 ==> 1
	292	1	0.333	0 ==> 1		79	1	0.500	0 ==> 1
Node 41 -->	36	1	0.286	1 ==> 0		83	3	0.200	0 ==> 3
<i>Paraceratherium</i>	89	1	0.250	2 --> 1		94	1	0.429	2 ==> 3
<i>transouralicum</i>	110	2	0.214	2 ==> 0		104	1	0.250	0 ==> 1
(Pavlow, 1922)	118	1	0.143	1 ==> 0		109	2	0.200	1 ==> 3
	121	1	0.167	1 ==> 0		111	1	0.500	0 ==> 1
	217	1	0.500	0 ==> 1		147	1	0.429	2 ==> 3
Node 42 -->	83	2	0.200	0 ==> 2		154	1	0.333	1 ==> 0
<i>Urtnotherium</i>	120	1	0.125	1 ==> 0		159	3	0.167	0 ==> 3
<i>intermedium</i>	151	3	0.300	3 ==> 0		294	1	0.250	0 --> 1
(Chiu, 1962)	161	1	0.400	1 ==> 0	Node 36 --> Node 35	18	1	0.500	0 --> 1
	252	1	0.500	2 --> 1		19	1	0.250	1 ==> 0
	254	1	0.200	0 ==> 1		20	1	0.286	1 --> 2
	261	2	0.333	2 --> 0		63	1	0.400	0 ==> 1
	289	1	0.167	1 ==> 2		143	1	0.500	1 ==> 0
	295	2	0.286	0 ==> 2		165	1	0.500	1 ==> 0
Node 40 -->	12	1	0.200	0 ==> 1		188	1	0.333	0 --> 1
<i>Hyrcodon</i>	19	1	0.250	1 ==> 2		199	1	0.333	0 --> 1
<i>nebraskensis</i>	34	1	0.167	0 ==> 1		218	1	0.500	0 ==> 1
(Leidy, 1850)	36	1	0.286	1 ==> 2		227	1	1.000	0 --> 1
	42	1	0.400	1 --> 0		242	1	1.000	1 ==> 0
	45	1	0.250	0 ==> 1		250	1	1.000	1 ==> 0
	46	1	0.500	0 ==> 1	Node 35 --> Node	10	1	0.167	1 --> 0
	54	1	0.333	1 ==> 0	<i>34 (Rhinocerotidae</i>	23	1	0.250	0 --> 1
	59	1	0.500	0 ==> 1	Gray, 1821)	44	1	0.333	0 ==> 1

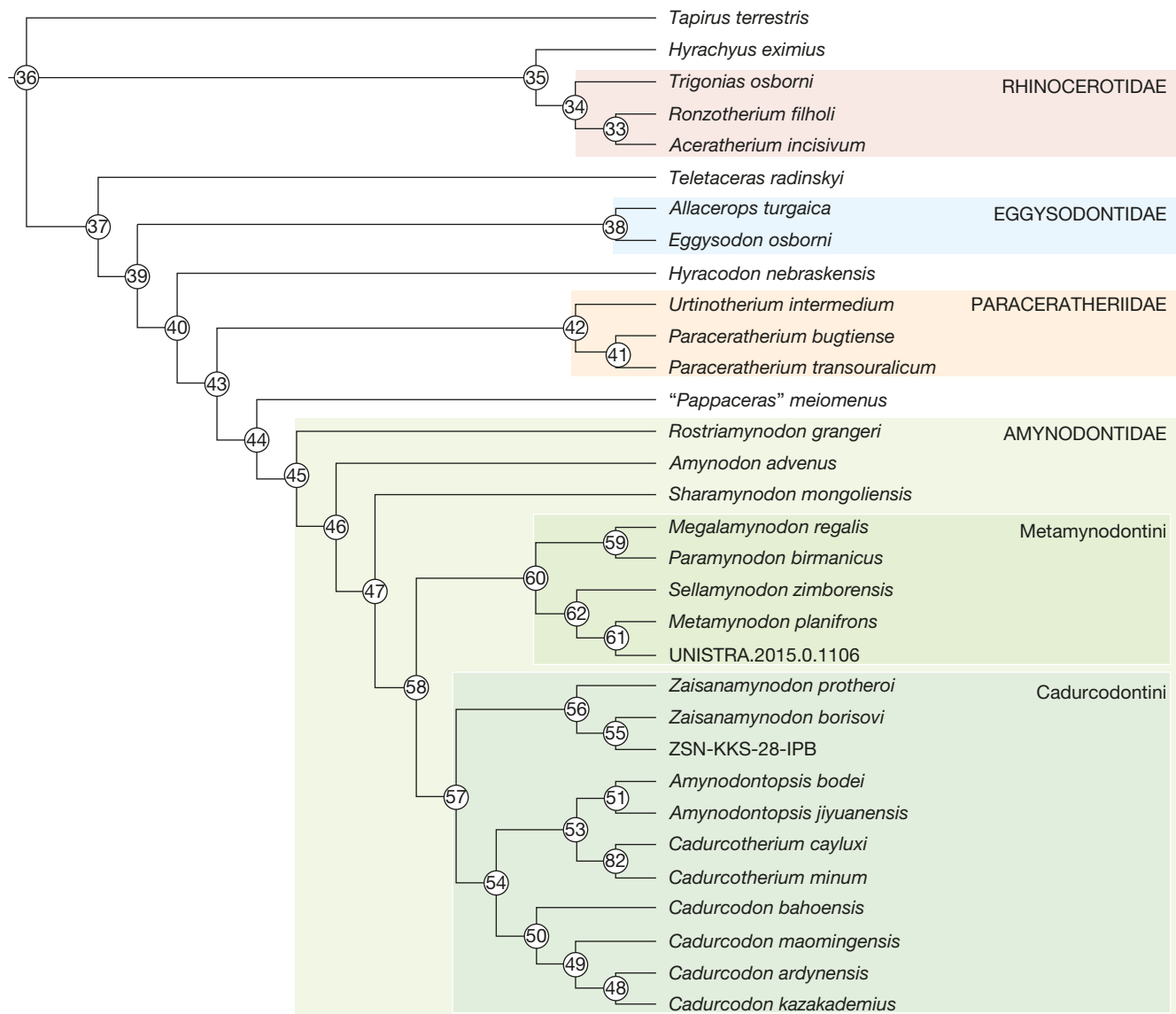
APPENDIX 4. — Continuation.

Branch	Character	Steps	CI	Change	Branch	Character	Steps	CI	Change	
	53	1	0.143	1 --> 2		61	1	0.333	0 ==> 1	
	79	1	0.500	0 ==> 1		63	1	0.400	1 ==> 0	
	81	1	0.250	0 ==> 1		94	1	0.429	2 ==> 1	
	82	1	0.500	0 ==> 1		102	1	0.333	2 ==> 3	
	102	1	0.333	0 --> 2		105	1	0.188	1 ==> 2	
	118	1	0.143	0 --> 1		108	1	0.250	1 ==> 0	
	154	1	0.333	1 ==> 0		112	1	0.333	1 ==> 2	
	159	2	0.167	0 --> 2		118	1	0.143	1 --> 0	
	191	1	0.500	0 --> 1		147	1	0.429	2 ==> 1	
	212	1	0.250	1 ==> 0		157	1	0.250	1 ==> 0	
	213	1	0.333	1 --> 0		159	2	0.167	2 --> 0	
	220	1	0.500	0 ==> 1		194	1	0.500	0 ==> 1	
	223	1	1.000	0 ==> 1		199	2	0.333	1 ==> 3	
	230	1	1.000	0 --> 1		218	1	0.500	1 ==> 0	
	252	1	0.500	0 ==> 1		230	1	1.000	1 ==> 2	
	253	1	0.500	0 ==> 1		238	1	0.333	1 --> 0	
	271	2	0.333	2 ==> 0		261	1	0.333	1 ==> 2	
	290	1	0.200	0 --> 1		265	1	0.667	0 ==> 1	
Node 34 --> <i>Trigonias osbornii</i> Lucas, 1900	1	1	0.500	0 ==> 1		17	1	1.000	0 ==> 1	
	6	1	0.500	0 ==> 1		19	1	0.250	0 ==> 1	
	47	1	0.667	0 ==> 1		23	1	0.250	1 --> 0	
	49	1	0.500	0 ==> 1		29	1	1.000	0 ==> 1	
	55	1	0.250	0 ==> 1		34	1	0.167	0 ==> 1	
	72	1	0.500	0 ==> 1		54	1	0.333	0 ==> 1	
	109	1	0.200	1 --> 0		86	1	0.333	0 ==> 1	
	149	1	0.333	0 ==> 1		95	1	0.250	0 ==> 1	
	174	1	1.000	0 ==> 1		99	1	0.143	1 --> 0	
	183	1	0.500	0 ==> 1		100	1	1.000	0 ==> 1	
	188	1	0.333	1 --> 0		101	2	1.000	0 ==> 2	
	199	1	0.333	1 --> 0		103	1	0.200	1 ==> 2	
	208	1	0.500	0 ==> 1		109	1	0.200	1 ==> 2	
	214	1	1.000	0 ==> 1		111	1	0.500	2 ==> 3	
	241	1	0.333	0 ==> 1		113	1	1.000	0 ==> 1	
	243	1	1.000	0 ==> 1		114	1	0.158	0 ==> 1	
	263	1	0.300	1 --> 0		115	3	1.000	0 ==> 3	
	266	1	1.000	0 ==> 1		122	1	0.500	0 ==> 1	
	282	1	1.000	0 ==> 1		125	1	1.000	0 ==> 1	
Node 34 --> Node 33	18	1	0.500	1 --> 0		129	1	1.000	0 ==> 1	
	20	1	0.286	2 --> 1		133	1	0.333	0 ==> 1	
	36	1	0.286	1 ==> 0		134	1	1.000	0 ==> 1	
	42	1	0.400	0 --> 1		135	2	1.000	0 ==> 2	
	58	1	1.000	0 --> 1		138	1	0.250	0 --> 1	
	74	1	0.250	0 ==> 1		140	1	0.400	1 ==> 0	
	75	1	0.500	0 ==> 1		142	1	0.333	0 ==> 1	
	89	1	0.250	0 ==> 1		146	1	0.333	0 ==> 1	
	105	1	0.188	0 ==> 1		150	1	0.250	0 ==> 1	
	107	1	0.750	0 ==> 1		151	1	0.300	0 ==> 1	
	110	1	0.214	1 ==> 2		152	2	0.333	0 ==> 2	
	111	2	0.500	0 ==> 2		160	1	0.250	0 --> 1	
	112	1	0.333	0 ==> 1		161	1	0.400	0 ==> 1	
	119	1	0.333	0 ==> 1		193	1	0.500	0 ==> 1	
	120	1	0.125	0 ==> 1		196	1	0.500	0 ==> 1	
	144	1	0.333	1 --> 0		201	1	0.333	0 ==> 1	
	157	1	0.250	2 ==> 1		204	1	1.000	0 ==> 1	
	222	2	1.000	0 --> 2		205	1	1.000	0 ==> 1	
	223	1	1.000	1 --> 2		206	1	1.000	0 ==> 1	
	228	2	0.500	0 ==> 2		207	1	0.333	0 ==> 1	
	258	1	0.500	0 ==> 1		210	1	1.000	0 ==> 1	
	261	1	0.333	0 ==> 1		213	1	0.333	0 --> 1	
	268	1	0.500	0 ==> 1		216	1	1.000	0 ==> 1	
	286	1	0.200	0 --> 1		224	1	0.500	0 ==> 1	
Node 33 --> <i>Ronzotherium filholii</i> (Osborn, 1900)	2	1	0.250	0 ==> 1		226	2	0.500	0 ==> 2	
	11	1	0.250	1 ==> 0		232	1	1.000	0 ==> 1	
	12	1	0.200	0 ==> 1		244	1	0.500	0 --> 1	
	15	1	0.500	0 ==> 1		245	1	0.500	0 ==> 1	
	20	1	0.286	1 ==> 0		251	1	1.000	0 ==> 1	
	35	1	0.500	0 ==> 1		254	1	0.200	0 ==> 1	
	37	1	0.143	0 ==> 1		Node 35 --> <i>Hyrrachys eximus</i> Leidy, 1871	16	1	0.333	1 --> 0
	53	2	0.143	2 --> 0		53	1	0.143	1 --> 0	
	56	1	0.167	1 ==> 0		60	1	0.286	1 ==> 2	

APPENDIX 4. — Continuation.

Branch	Character	Steps	CI	Change
	83	1	0.200	0 ==> 1
	94	1	0.429	2 ==> 0
	98	1	0.250	0 ==> 1
	104	1	0.250	0 ==> 1
	109	1	0.200	1 ==> 2
	110	1	0.214	1 --> 0
	121	1	0.167	0 ==> 1
	147	1	0.429	2 ==> 3
	184	1	0.500	1 --> 0
	196	1	0.500	0 ==> 1
	199	2	0.333	1 ==> 3
	201	1	0.333	0 ==> 1
	207	1	0.333	0 ==> 1
	211	1	0.333	0 ==> 1
	263	2	0.300	1 ==> 3
	272	1	0.500	0 ==> 1
	275	1	0.333	0 ==> 1

APPENDIX 5. — Single parsimonious tree of Amynodontidae Scott & Osborn, 1883 within Rhinocerotoidea Owen, 1845, with *Tapirus terrestris* (Linnaeus, 1758) and *Hyracetus eximius* Leidy, 1871 considered as outgroups. Tree length = 805; CI = 0.3938; RI = 0.4906. Numbers inside white circles are node numbers.



APPENDIX 6. — List of occurrences of *Amynodontopsis* Stock, 1933, *Cadurcotherium* Gervais, 1873, *Metamynodon* Scott & Osborn, 1887, *Zaisanamynodon* Belyaeva, 1971 and other genera of Amynodontidae Scott & Osborn, 1883 in Asia, Europe, and North America, range from middle Eocene to late Oligocene.

Ages	Taxa	Countries	Localities	References
Oligocene late	<i>Cadurcotherium</i> Gervais, 1873	Bosnia and Herzegovina	Ugljevik	Malez & Thenius (1985)
		Pakistan	Bugti Hills	Antoine et al. (2004)
	Other	Kazakhstan	Akespe	Birjukov (1961); Lucas & Emry (1996)
	<i>Cadurcotherium</i>	France	Aubenas-les-Alpes Briatexte, Tarn Le Garouillas, Tarn-et-Garonne Rigal-Jouet, Tarn-et-Garonne	Ménouret et al. (2015) Roman & Joleaud (1909) De Bonis (1995) Ménouret (2018)
		Spain	Carrascosa del Campo	Crusafont Pairó & Aguirre (1973)
	Other	Kazakhstan	Kalmakpay Mountain, Zaysan Basin Myneske-Suyek, Dzhilanchik Basin	Russell & Zhai (1987); Lucas & Emry (1996); Emry et al. (1998)
	<i>Cadurcotherium</i>	France	Barrières, Haute-Loire Dausse, Lot-et-Garonne	Birjukov (1961); Russell & Zhai (1987); Lucas & Emry (1996)
			Etampes, Essonne Isle-sur-Sorgue, Vaucluse Moissac, Tarn-et-Garonne Puylaurens, Tarn Pech Crabit, Lot	Ménouret (2018) Roman & Joleaud (1909)
		Germany	Vendèze, Cantal	Ménouret (2018)
	<i>Metamynodon</i> Scott & Osborn, 1887	Switzerland	Weinheim-Alzey	Ménouret (2018)
		United States	Bressaucourt, Canton du Jura	Becker (2009)
			North Dakota	Wall (1998)
			South Dakota	Wall (1998); This study
?late Eocene- ?early Oligocene	Other	China	Bassin Lunan and Yuezhou, Yunnan Province	Xu (1966); Russell & Zhai (1987)
			Suhaitu, Haosibuerdu Basin, Inner Mongolia	
			Sunid Zuqi, Inner Mongolia	Russell & Zhai (1987)
		Kazakhstan	Kii Kerish III, Zaysan Basin	Russell & Zhai (1987); Emry et al. (1998)
		Mongolia	Dzamyn Ude	Dashzeveg (1996)
			Ergilin-Dzo and Khoer-Dzan, Gua-Teg, Dornogobi Province	Russell & Zhai (1987)
			Lantian Basin, Shaanxi Province	Xu (1965); Russell & Zhai (1987)
		Romania	Dobârca	Tissier et al. (2018)
	<i>Amynodontopsis</i>	Chine	Urtyn Obo, Ulan Gochu (Inner Mongolia)	Wall (1980); Wang (1992)
		Mexico	Bassin Tlaxiaco	Jiménez-Hidalgo et al. (2015)
Eocene late	<i>Amynodontopsis?</i>	Romania	Morlaca	Tissier et al. (2018)
	<i>Metamynodon</i>	United States	South Dakota	Gillet (1960); Wall (1998)
			Mississippi	
			Texas	
	<i>Zaisanamynodon</i>	China	Ulan Shireh Obo, Baron Sog Lamasery, Urtyn Obo (Inner Mongolia)	Lucas et al. (1996)
		Japan	Tatsukawa Colliery, Imari City, Saga	Miyata et al. (2011)
		Kazakhstan	Kii Kerish II, Zaysan Basin	Belyaeva (1971); Russell & Zhai (1987); This study
	Other	Bulgaria	Nikolaev, Kameno	Nikolov & Heissig (1985)
		China	Jiyan Basin, Henan Province	Russell & Zhai (1987)
			Wucheng Basin, Henan Province	Young (1937); Russell & Zhai (1987)
middle-late middle			Yuanqu Basin, Shanxi Province	Chow & Xu (1965)
			Lushi, Henan Province	
			Mianchi, Henan Province	
			Tientong, Guangxi	Chow (1957)
			Ula Usu, Inner Mongolia	Osborn (1936); Xu (1966)
		Hungary	Tápiószele	Kretzoi (1940)
		Japan	Karatsu	Tomida & Yamakasi (1996)
		China	Maoming Basin	Averianov et al. (2016)
		China	Jiyan Basin, Henan Basin	Wang et al. (2020)
	<i>Amynodontopsis</i>	United States	California	Wall (1998)
			Montana	

APPENDIX 6. — Continuation.

Ages	Taxa	Countries	Localities	References
			Texas	
			Utah	
			Wyoming	
	<i>Amynodontopsis?</i>	Hungary	Dorog	Tissier et al. (2018)
	<i>Metamynodon</i>	United States	Texas	Wall (1998)
	<i>Zaisanamynodon</i>	United States	Oregon	Lucas (2006)
		Russia	Artyom	Gromova (1960); Lucas (2006)
Other		China	Baise Basin, Guangxi	Russell & Zhai (1987)
			Lijiang Basin, Yunnan Province	Russell & Zhai (1987)
			Xichuan Basin, Henan Province	Russell & Zhai (1987)
			Camp Margetts Area, Inner Mongolia	Wall & Manning (1986)
			Liankan, Turpan Basin, Xinjiang	Russell & Zhai (1987)
			Uygur	
			Mengjiapo, Lushi Basin, Henan Province	Chow & Xu (1965); Russell & Zhai (1987)
			North Mesa, Ulan Shireh, Inner Mongolia	Xu (1966); Russell & Zhai (1987)
			Rencun, Henan Province	Huang & Wang (2001)
			Tongbai, Wucheng Basin, Henan Province	Russell & Zhai (1987)
		Kazakhstan	Weinan, Shaanxi Province	Li (2003)
		Kyrgyzstan	Kyzyl Murun	Lucas & Emry (2001)
		Myanmar	Andarak 2	Averianov & Godinot (2005)
		United States	Mogaung + Myaing	Colbert (1938); Russell & Zhai (1987)
			Montana	Wall (1998)
			Utah	